

Atomic H over plane: effective potential and level reconstruction

S. Artyukova,^{1,*} K. Sveshnikov,^{1,†} and A. Tolokonnikov^{1,‡}

¹*Department of Physics and Institute of Theoretical Problems of MicroWorld,
Moscow State University, 119991, Leninsky Gory, Moscow, Russia*

(Dated: January 29, 2019)

The behavior of atomic H in a semi-bounded space $z \geq 0$ with the condition of “not going through” the boundary (the surface $z = 0$) for the electronic wavefunction (WF) is considered. It is shown that in a wide range of “not going through” condition parameters the effective atomic potential, treated as a function of the distance h from H to the boundary plane, reveals a well pronounced minimum at certain finite but non-zero h , which describes the mode of “soaring” of the atom above the plane. In particular cases of Dirichlet and Neumann conditions the analysis of the soaring effect is based on the exact analytical solutions of the problem in terms of generalized spheroidal Coulomb functions. For h varying between the regions $h \gg a_B$ and $h \ll a_B$ both the deformation of the electronic WF and the atomic state are studied in detail. In particular, for the Dirichlet condition the lowest $1s$ atomic state transforms into $2p$ -level with quantum numbers 210, the first excited ones $2s$ — into $3p$ with numbers 310, $2p$ with $m = 0$ — into $4f$ with numbers 430, etc. At the same time, for Neumann condition the whole picture of the levels transmutation changes drastically. For a more general case of Robin (third type) condition the variational estimates, based on special type trial functions, as well as the direct numerical tools, realized by pertinent modification of the finite element method, are used. By means of the latter it is also shown that in the case of a sufficiently large positive affinity of the atom to the boundary plane a significant reconstruction of the lowest levels takes place, including the change of both the asymptotics and the general dependence on h .

PACS numbers: 31.15.A-, 32.30.-r, 34.35.+a, 37.30.+i

Keywords: confined quantum systems, Robin condition, atomic H over plane, soaring effect, level reconstruction, hydrogenation

1. INTRODUCTION

Considerable amount of theoretical and experimental activity has been focused recently on spatially confined atoms and molecules [1–3]. The interest is largely due to the nontrivial physical and chemical properties that arise for quantum systems in such a state of complete or incomplete confinement. The interaction of confined particles with the environment, forming the cavity or volume boundary, is usually simulated by means of a suitable boundary condition, imposed on their wavefunctions (WF). The pioneering works on quantum system in a closed cavity are the Wigner-Seitz model [4, 5] and the papers [6] and [7] on atomic H in a spherical cavity. More concretely, in the Wigner-Seitz model the metallic bond formation in alkali metals has been considered in terms of the Neumann condition for the valence electron on the boundary of the corresponding Wigner-Seitz cell. In Ref. [6] the exact solution for atomic H in a spherical cavity with the Dirichlet boundary condition was found, while in Ref. [7] such a model has been used for description of atomic H under high pressure.

Atoms in the Euclidean half-space $\mathcal{R}^3/2$ have been first explored in Ref. [8], devoted to the properties of the impurity donor atom placed on the plane boundary of the dielectric crystal. Due to a large positive affinity it is en-

ergetically favorable for the valence electron to reside inside the crystal that allows to simulate the crystal boundary by means of the Dirichlet condition imposed on the electronic WF. Afterwards, this model has been actively used by solving the spectral problem for an atom, placed inside a semiconductor near its surface. In contrast to the one considered in Ref. [8], in the latter case the analytic solution of the Schroedinger eq. (SE) is absent, therefore various numerical tools are used (see, e.g., Refs. [9–12]).

Further research was not limited to the study of spherical cavities or plane boundaries, rather it was motivated by the circumstance that SE with Coulomb potential allows for separation of variables not only in spherical, but also in spheroidal and parabolic frames. Therefore besides a sphere [4–7] and plane [8–12] there have been considered other “natural” for the above-mentioned frames surfaces, namely, elliptic cones, plane angles, etc. (see Refs. [13–19] and refs. therein), with impenetrable [9–19] or semipermeable [20, 21] potential wall used as a boundary. It should be mentioned, however, that for such problems the explicit analytic solution in a closed form is actually impossible, since the answers are formulated in terms of convergent infinite series, and so practically meaningful calculations are restricted to a finite number of first terms in these series [9–21].

The behavior of atomic He and of He⁺ ion in a half-space with plane boundary [12] has been studied experimentally [22, 23]. However, the performed experiments have shown that the levels shift in He depends not only on the distance to the boundary (that could be described within the idealized model with the Dirichlet boundary condition), but also on the crystal structure of matter

*Electronic address: s.artyukova@physics.msu.ru

†Electronic address: costa@bog.msu.ru

‡Electronic address: tolokonnikov@physics.msu.ru

(Al and noble metals) that forms this boundary. The Dirichlet condition cannot in principle take account for such effects, since it nullifies the electronic WF on the boundary. At the same time, the general boundary conditions of “not going through” (i.e., Robin, or third kind) allow for a sufficiently more wide problem statement, which doesn’t imply the vanishing WF on the volume boundary [24–32]. Moreover, such conditions are able to take into account the interaction of confined particles with medium, surrounding the cavity or demarcating the half-space [28–31], [33, 34]. It would be worth to note that the term “not going through”, used here, underlines that these conditions do not necessarily originate from the actual confinement of particles inside the given volume, rather they may be caused by a significantly wider number of reasons, as it takes place, in particular, in the Wigner-Seitz model of an alkali metal [4, 5], where the valence electron state is principally delocalized. The latter circumstance turns out to be quite important, since in some cases the cavities, where a particle or an atom could reside, form a lattice, similar to that of an alkali metal, like certain interstitial sites of a metal supercell, e.g. next-to-nearest octahedral positions of palladium fcc lattice [35]. In this case a particle (or a valence electron, provided that the whole lattice of cavities is occupied by identical atoms) finds itself in a periodic potential of a cubic lattice, and so the description of its ground state could be based on the first principles of the Wigner-Seitz model [30, 31], [33, 34].

In the present paper the behavior of atomic H in the half-space $z \geq 0$ with the plane boundary $z = 0$, whereon the electronic WF should be subject of the general Robin condition, is studied in the adiabatic approximation with respect to nucleus motion. The main motivation is that if H is inside a spherical cavity with the radius R and a δ -like potential on its border, which simulates the interaction of atomic electron with medium, wherein the cavity is formed, then for a wide range of surface interaction coupling constant (including repulsion!) with growing R the equilibrium position of the atom in the center of cavity ceases to be stable and it shifts to the border [33, 34]. When the curvature of the border becomes much larger than a_B , then the problem of an H over plane with Robin boundary condition for the electronic WF appears in a natural way. In this problem there are two most important questions. The first one is under which conditions imposed on the surface interaction the effective atomic potential treated as a function of the distance h to the plane reveals a minimum for finite and nonzero h . A preliminary, rather rough estimate for this effect has been considered in Refs.[33, 34]. The second concerns the additional “power-like” levels, which appear always under Robin boundary condition with attractive surface interaction and become the lowest ones, when the attraction is sufficiently strong. Here we’ll present a detailed study of both questions.

The paper is organized as follows. In Section 2 the general problem statement for atomic H over plane is presented, supplied with the required information for further

analysis from the similar problem in a spherical cavity. In Section 3 the partial cases of the general “not going through” condition, namely, the Dirichlet and Neumann ones, which allow for a “quasi-exact” analysis of the problem, are considered. There are explored in detail the ground state and two first excited levels “2s” and “2p”. In Section 4 special kind trial functions, which allow for qualitative reproduction of the analytic results for the Neumann condition, as well as of the results of direct numerical calculations for the Robin case, with additional restriction on the magnitude of attractive surface interaction from above, are considered. In Section 5 a sufficiently more wide range of the magnitude of surface interaction is explored. The numerical results for the lowest levels are presented and compared, if possible, with those achieved via variational estimates. Special attention is paid to additional “power-like” levels, which come into play for sufficiently strong attractive surface interaction. In Conclusion (Section 6) the main consequences of the atomic H “soaring” effect and lowest levels reconstruction in the case of sufficiently strong positive electron-plane affinity are discussed.

Throughout the paper the a. u. $\hbar = m = e = 1$, Computer Algebra Systems (such as Maple 18) to facilitate the analytic calculations and GNU Octave code for boosting the numerical work, are used.

2. THE PROBLEM STATEMENT FOR ATOMIC H IN $\mathbb{R}^3/2$

The initial formulation of the problem repeats almost completely the one, considered in Refs.[24–32]. In the present case the energy functional for the electronic WF takes the form

$$E[\psi] = \int_{z \geq 0} d\vec{r} \left[\frac{1}{2} |\vec{\nabla} \psi|^2 + V(\vec{r}) |\psi|^2 \right] + \frac{1}{2} \int_{z=0} d\vec{\rho} \lambda(\vec{\rho}) |\psi|^2, \quad (1)$$

where

$$V(\vec{r}) = -1/\sqrt{\rho^2 + (z-h)^2} \quad (2)$$

is the Coulomb potential of the nucleus (the proton) with coordinates $(0, 0, h)$, while the surface term describes the interaction of the atomic electron on the border $z = 0$, demarcating the half-space $z > 0$, with medium, filling another half-space with $z < 0$. The concrete properties of this surface interaction are determined via a real-valued function $\lambda(\vec{\rho})$.

Proceeding further, from the variational principle one obtains

$$\left[-\frac{1}{2} \Delta + V(\vec{r}) \right] \psi = E\psi \quad (3)$$

for $z > 0$ and the boundary condition on the surface $z = 0$

$$\left[\partial/\partial z - \lambda(\vec{\rho}) \right] \psi \Big|_{z=0} = 0. \quad (4)$$

The “not going though” property is fulfilled here via vanishing normal to the surface component of the quantum-mechanical flux \vec{j}

$$j_z|_{z=0} = 0. \quad (5)$$

At the same time, the tangential components of \vec{j} could be remarkably different from zero on the surface $z = 0$ and so the atomic electron could be found quite close to the boundary with a marked probability.

When $\lambda = 0$, the interaction of the atom with environment is absent and so eq. (4) transforms into Neumann (second kind) condition

$$\partial\psi/\partial z|_{z=0} = 0. \quad (6)$$

If $\lambda \rightarrow \infty$, then (4) transforms into the Dirichlet condition

$$\psi|_{z=0} = 0, \quad (7)$$

and hence, describes confinement by an impenetrable barrier.

Here it should be noted that the interaction of atomic electron with environment by means of the surface δ -potential is a simplification of the actual situation, since in this picture the atomic structure of medium is disregarded. So the different type surface excitations and inside the bulk don't be taken into account explicitly, rather they are involved into the properties of the boundary condition. However, to the first approximation such description turns out to be satisfactory, because it allows for qualitative accounting for such general features as the atomic H affinity to medium, surrounding the cavity or demarcating the half-space. The general literature on the interaction of atomic H with surfaces of different nature is extremely vast, since it includes such interdisciplinary aspects as hydrogenation, dehydrogenation, and hydrogenolysis processes that are crucially important to the chemical industry. A thorough review of this literature is beyond the scope of the present paper (for a detailed summary of older hydrogen literature, the reader is referred to excellent reviews presented in Refs.[36–38]). More recent studies on this subject are considered in Refs.([39–42] and citations therein). The nowadays most efficient self-consistent methods for the study of various properties of both surface and subsurface atomic hydrogen are based mostly on Gradient corrected periodic density functional theory (DFT-GGA) slab calculations [43–47]. Very roughly, the averaged affinity estimates (ignoring both the difference between physisorption and chemisorption and the dependence on the current concentration of H in the bulk), found this way for atomic H in terms of λ , vary from very large positive values (liquid He) to large negative ones in PdH_x and TiH_x, provided $x \ll 1$.

A simple example for estimating λ follows directly from the well-known quantum-mechanical problem of a particle in the δ -potential $V(\vec{r}) = (\lambda/2) \delta(r - R)$ [48, 49]. In this case the ground state WF $u_0(r) = rR_0(r)$ up to

normalization coefficient takes the form

$$\begin{aligned} u_0(r) &= \sqrt{\frac{r}{R}} K_{1/2}(\beta R) I_{1/2}(\beta r) = \\ &= \frac{\exp(-\beta R)}{\beta R} \sinh(\beta r), \quad r \leq R, \\ u_0(r) &= \sqrt{\frac{r}{R}} I_{1/2}(\beta R) K_{1/2}(\beta r) = \\ &= \frac{\sinh(\beta R)}{\beta R} \exp(-\beta r), \quad r > R, \end{aligned} \quad (8)$$

with $I_{1/2}(z)$ and $K_{1/2}(z)$ being the modified Bessel functions, $\beta = \sqrt{2I}$, while $I = -E$ is the electron affinity energy to the source of the δ -potential. The relation between λ and the parameters I and R , which are determined experimentally, is obtained from the jump in the logarithmic derivative at $r = R$

$$\beta(1 + \coth(\beta R)) = -\lambda. \quad (9)$$

In particular, for the negatively charged fullerene ion C_{60}^- one has $R = 6.639 a_B$ and $I = 2.65 eV = 0.097 Ha$ [48, 49], whence $\lambda = -0.885 Ha \times a_B$. The additional electron in C_{60}^- the most part of time resides in those spatial regions, where its interaction with C_{60} is negligibly small, that allows to find the electronic WF in almost the whole space without detailed information on the true C_{60} potential. Translating this result to our problem, we get the estimate for λ in (1) as $\pm O(1)$ in units $Ha \times a_B$, which is consistent with results for a large set of transition metals and near-surface alloys [47].

From the beginning the problem for the energy levels of atomic H in $\mathfrak{R}^3/2$ with the boundary condition (4) requires for taking into account the following circumstance. Because this problem partially (but not completely!) could be considered through the limit $R \rightarrow \infty$ of the similar problem for atomic H, confined to a spherical cavity of radius R with the same boundary condition, the energy levels of H in a cavity should possess their analogues in $\mathfrak{R}^3/2$. The complete correspondence here is absent, since in a spherical cavity with the nucleus placed in the center for any R the orbital moment is conserved and so the eigenstates of H are labeled by the quantum numbers lm , although the additional degeneration of levels disappears [26, 27]. In $\mathfrak{R}^3/2$ for any finite distance h between the nucleus and the boundary plane $z = 0$ there remains only the axial symmetry, hence, the only conserved quantity is l_z . In a cavity with finite R such situation also takes place when the equilibrium position of H shifts from the center to the border, that happens whenever $\lambda < q$ with q being the nucleus charge [33, 34]. In $\mathfrak{R}^3/2$ the spherical symmetry restores only for infinite distances between the atom and plane and only in the case, when the atomic electron is localized in the nucleus vicinity, where it falls into the eigenstates of the free atom. But this is not the general case. Namely, for $\lambda < 0$ atomic H in a spherical cavity with finite R acquires a set of qualitatively different levels, when the electron is partially (but not completely) localized in the vicinity of

the border [30, 31, 33, 34]. These states are orthogonal to the “normal” atomic states, in which the electron is localized in the nucleus vicinity, and together they form the complete set of states of atomic H, trapped into a cavity, for $\lambda < 0$. Moreover, these additional states reveal a number of principally different features, which show up most clearly in their asymptotic behavior for large separation between nucleus and the border, which turns out to be a power-like one with the common limiting point $(-\lambda^2/2)$. These levels possess their own analogues in $\mathfrak{R}^3/2$, when the atomic electron is partially (but not completely) localized in the neighborhood of the boundary plane, and are qualitatively different from the “normal” levels, corresponding to the electron localization in the nucleus vicinity. Most clearly this difference shows up in the dependence of these levels on h for $h \rightarrow \infty$.

Since a large number of problems concerning the one-electron atom with the nucleus charge q , trapped into a spherical cavity of radius R with the Robin condition, has been already considered in Refs.[24–32], here only a certain detail clarification is required. Quite similar to the previous example with C_{60} , we’ll imply here that the surface interaction is determined by a constant λ , while the motionless point-like atomic nucleus is placed in the center of cavity, hence, the spherical symmetry is maintained. From the solution of the Schroedinger-Coulomb problem for the radial electronic WF with the orbital momentum l one obtains up to a numerical factor

$$R_l(r) = e^{-\gamma r} r^l \Phi(b_l, c_l, 2\gamma r), \quad (10)$$

where

$$\gamma = \sqrt{-2E}, \quad b_l = l + 1 - q/\gamma, \quad c_l = 2l + 2, \quad (11)$$

with $\Phi(b, c, z)$ being the confluent hypergeometric function of the first kind (Kummer function). Definition, notations and main properties of the Kummer function follow Ref.[50]. The energy levels with the orbital momentum l are determined from the equation

$$[q/\gamma + (\lambda - \gamma)R - 1] \Phi_R + [l + 1 - q/\gamma] \Phi_R(b+) = 0, \quad (12)$$

where

$$\Phi_R = \Phi(b_l, c_l, 2\gamma R), \quad \Phi_R(b+) = \Phi(b_l + 1, c_l, 2\gamma R). \quad (13)$$

The reconstruction of the electronic spectrum in the cavity shows up most clearly for $R \rightarrow \infty$, when by means of the asymptotics of Φ_R , $\Phi_R(b+)$ one obtains from (12), that besides the “normal” discrete spectrum of the free atom in the case of attractive surface interaction with $\lambda < 0$ there emerges another set of levels $\tilde{E}_l(R)$ with a power-like asymptotics for $R \rightarrow \infty$ and a common limiting point $\tilde{E}_l(\infty) = -\lambda^2/2$, namely

$$\begin{aligned} \tilde{E}_l(R) &\rightarrow -\lambda^2/2 + (\lambda - q)/R + \\ &+ (l(l+1) - 1 + q/\lambda)/R^2 + O(1/R^3), \quad R \rightarrow \infty. \end{aligned} \quad (14)$$

It should be mentioned that for $\lambda < -q < 0$ these levels become the lowest ones for any R and as functions of R

behave similar to the lowest level of a particle confined to a spherical cavity [30], namely, $\tilde{E}_l(R)$ have the form of hyperbolas shifted down relative to the x-axis. The lowest one in this bundle of power levels with different l will be quite naturally the s -level with $l = 0$, while all the others with $l \neq 0$ will be raised higher in proportion to their centrifugal energy.

At the same time, the “normal” atomic states tend for $R \rightarrow \infty$ to the values, which make up the discrete spectrum of free H. Moreover, they approach these values exponentially fast, since their asymptotics is created by approaching the argument of the factor $\Gamma^{-1}(b)$, entering the asymptotics of the Kummer function $\Phi(b, c, z)$, to the pole $b \rightarrow -n_r$, $n_r = 0, 1, \dots$. It would be worth to emphasize here once more that for atomic H in the cavity with the Robin boundary condition the Runge-Lenz vector is no longer conserved [26, 27], therefore these levels should be labeled now with two quantum numbers $n = n_r + 1$ and l .

In particular, for the “normal” ns -levels one finds

$$\begin{aligned} E_{n0}(R) - E_{n0} &\rightarrow \\ \frac{\lambda - \gamma_{n0}}{\lambda + \gamma_{n0}} \left[\frac{\gamma_{n0}}{n!} \right]^2 &(2\gamma_{n0}R)^{2n} e^{-2\gamma_{n0}R}, \quad \gamma_{n0}R \gg 1, \end{aligned} \quad (15)$$

where

$$E_{n0} = -\gamma_{n0}^2/2, \quad \gamma_{n0} = q/n, \quad n = 1, 2, \dots, \quad (16)$$

are the electronic ns -levels of the free atom. Remark, that levels with $\gamma_{n0} < \lambda$ should approach their asymptotics from above, while those with $\gamma_{n0} > \lambda$ from below.

If $\lambda = \pm\gamma_{n0}$, the asymptotics (15) modifies in the next way. The exponential behavior is preserved, while the non-exponential factor undergoes changes in such a way, that the levels approach their asymptotics of the free atom only from above. For $\lambda = \gamma_{n0}$ their asymptotics takes the form

$$\begin{aligned} E_{n0}(R) - E_{n0} &\rightarrow (n-1) \left[\frac{\gamma_{n0}}{n!} \right]^2 (2\gamma_{n0}R)^{2(n-1)} e^{-2\gamma_{n0}R}, \\ &\gamma_{n0}R \gg 1, \end{aligned} \quad (17)$$

while for the lowest level $E_{10}(R)$ the exponential part disappears completely, since in this case $\lambda = \gamma_{10} = q$ and $E_{10}(R) = E_{1s} = -q^2/2$.

For $\lambda = -\gamma_{n0} < 0$ instead of (15) one obtains

$$\begin{aligned} E_{n0}(R) - E_{n0} &\rightarrow \\ \frac{1}{n+1} \left[\frac{\gamma_{n0}}{n!} \right]^2 &(2\gamma_{n0}R)^{2(n+1)} e^{-2\gamma_{n0}R}, \quad \gamma_{n0}R \gg 1. \end{aligned} \quad (18)$$

Moreover, in this case the limiting point of the level $\tilde{E}_0(R)$ with the power asymptotics (14) coincides with the corresponding level of the free atom (16), that in turn represents a remarkable example of von Neumann-Wigner avoided crossing effect, i.e. near levels reflection under perturbation [51–53] — infinitely close to each

other for $R \rightarrow \infty$ levels $E_{n0}(R)$ and $\tilde{E}_0(R)$ should for decreasing R diverge in opposite directions from their common limiting point E_{n0} . As a perturbation here serves the nucleus Coulomb field, since under Robin condition the electronic WF doesn't vanish on the cavity border, and so for $R \gg a_B$ the maximum of electronic density shifts to the region of large distances between the electron and nucleus, where the contribution of the Coulomb field is negligibly small compared to boundary effects. When R decreases, the Coulomb field increases, hence, $E_{n0}(R)$ should go upwards according to (18), while $\tilde{E}_0(R)$ goes downwards according to asymptotics

$$\tilde{E}_0(R) \rightarrow E_{n0} - \frac{n+1}{n} \frac{q}{R} + O(1/R^2), \quad R \rightarrow \infty. \quad (19)$$

As a result, in a spherical cavity under Robin condition and nucleus in the center: i) for $\lambda = q$ the lowest level of the one-electron atom $E_0(R)$ acquires for any R the constant value E_{1s} of the free atom; ii) for $\lambda > -q$ and $R \gg a_B$ it approaches E_{1s} exponentially fast; iii) for $\lambda \leq -q < 0$ it transforms into the level $\tilde{E}_0(R)$ with the power-like asymptotics (14), which in the whole range of R behaves similar to a hyperbole [30, 31].

Proceeding further, we'll see that all the above-mentioned effects, even the last one, one way or another manifest themselves for atomic H over plane.

3. EXACTLY SOLVABLE CASES FOR ATOMIC H OVER PLANE

For atomic H over plane there exist three partial cases, when the corresponding spectral problem (3), (4) allows for either exact or "quasi-exact" analytic solution. The first one is the already mentioned above result [24, 25, 28–31], well-known in quantum chemistry, that if the nucleus charge q and the surface interaction constant are related via $\lambda = q$, then for such one-electron atom in a spherical cavity of radius R for any $0 < R \leq \infty$ the lowest s -level is given by the exact solution of SE for the $1s$ state of the free atom, that means

$$E_{10}(R) = E_{1s} = -q^2/2. \quad (20)$$

The nucleus in this case resides exactly in the cavity center without displacement. So by passing to the limit $R \rightarrow \infty$ one obtains the exact solution for the lowest eigenstate of atomic H over plane with the coupling constant $\lambda = 1$, which implies that the atom has pushed off from the plane to infinity. In turn, it means that for $\lambda \geq 1$ the mutual reflection between H and plane should be so strong, that the minimal energy can be reached only for infinite removal of H from the plane.

Two other cases, which allow for a "quasi-exact" solution, correspond to Dirichlet ($\lambda \rightarrow +\infty$) and Neumann ($\lambda = 0$) boundary conditions. For these purposes let us pass to prolate spheroidal coordinates (ξ, η, φ) , $1 \leq \xi \leq \infty$, $-1 \leq \eta \leq 1$, $0 \leq \varphi < 2\pi$, in which the nucleus resides in the focus with coordinates $\xi = 1$ and $\eta = 1$,

while the boundary plane $z = 0$ is described by the condition $\eta = 0$. In this coordinate frame the Dirichlet and Neumann boundary conditions take the form

$$\psi \Big|_{\eta=0} = 0 \quad \text{and} \quad \frac{\partial \psi}{\partial \eta} \Big|_{\eta=0} = 0, \quad (21)$$

respectively, while SE allows for separation of variables [54].

Implying that $\psi = \Pi(\xi) \Xi(\eta) e^{\pm im\varphi}$, from (3) one obtains

$$\begin{aligned} \frac{d}{d\xi}(\xi^2 - 1) \frac{d}{d\xi} \Pi + \left[-\mu - p^2(\xi^2 - 1) + a\xi - \frac{m^2}{\xi^2 - 1} \right] \Pi &= 0, \\ \frac{d}{d\eta}(1 - \eta^2) \frac{d}{d\eta} \Xi + \left[\mu - p^2(1 - \eta^2) + b\eta - \frac{m^2}{1 - \eta^2} \right] \Xi &= 0, \end{aligned} \quad (22)$$

where μ is the separation parameter, $p^2 = -2Eh^2$ and $a = b = 2h$. The corresponding eigenfunctions are sought in the form of the following power series [54]

$$\Pi(\xi) = (\xi^2 - 1)^{m/2} e^{-p(\xi-1)} (\xi + 1)^\sigma \sum_{s=0}^{\infty} g_s x^s, \quad (23)$$

$$\Xi(\eta) = (1 - \eta^2)^{m/2} e^{-p(1-\eta)} \sum_{s=0}^{\infty} c_s (1 - \eta)^s,$$

where $\sigma = 1/\sqrt{-2E} - (m+1)$, while $x = (\xi - 1)/(\xi + 1)$. The expansion coefficients g_s and c_s are subject of the three-term recurrence relations

$$\begin{aligned} \omega_s g_{s+1} - \tau_s g_s + \gamma_s g_{s-1} &= 0, \\ \rho_s c_{s+1} - \kappa_s c_s + \delta_s c_{s-1} &= 0, \end{aligned} \quad (24)$$

wherein $g_{-1} = c_{-1} = 0$, while

$$\begin{cases} \omega_s = (s+1)(s+m+1), \\ \tau_s = 2s(s+2p-\sigma) - (m+\sigma)(m+1) - 2p\sigma + \mu, \\ \gamma_s = (s-1-\sigma)(s-m-1-\sigma), \\ \rho_s = 2(s+1)(s+m+1), \\ \kappa_s = s(s+1) + (2s+m+1)(2p+m) - b - \mu, \\ \delta_s = 2p(s+m) - b. \end{cases} \quad (25)$$

The conditions of regularity for $\Pi(\xi)$ on the interval $1 \leq \xi \leq \infty$ and $\Pi(\xi) \rightarrow 0$ for $\xi \rightarrow \infty$ lead to relation

$$\begin{vmatrix} -\tau_0 & \omega_0 & 0 & 0 & \dots \\ \gamma_1 & -\tau_1 & \omega_1 & 0 & \dots \\ 0 & \gamma_2 & -\tau_2 & \omega_2 & \dots \\ \dots & \dots & \dots & \dots & \dots \end{vmatrix} = 0, \quad (26)$$

while the Dirichlet and Neumann boundary conditions (21) take the form

$$\Xi(\eta) \Big|_{\eta=0} = 0 \Leftrightarrow \sum_{s=0}^{\infty} c_s = 0, \quad (27)$$

$$\frac{\partial \Xi(\eta)}{\partial \eta} \Big|_{\eta=0} = 0 \Leftrightarrow \sum_{s=0}^{\infty} (p-s)c_s = 0, \quad (28)$$

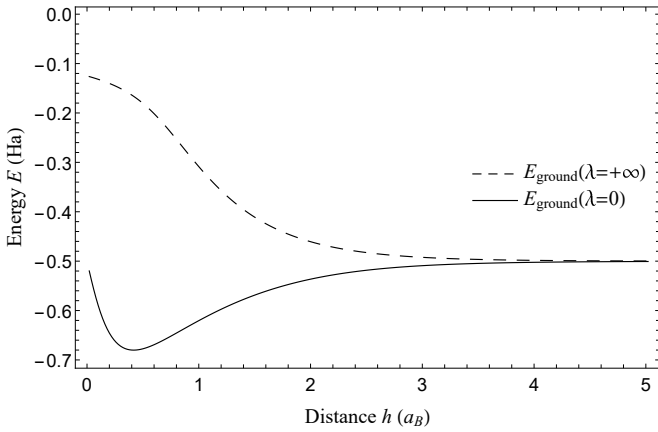


FIG. 1: Atomic H ground state energy $E(h)$ for the Dirichlet (dashed line) and Neumann (solid line) conditions.

respectively.

So upon cutting the series from above at certain finite s_{max} the search for the energy levels reduces to solution of the systems of algebraic equations (26), (27) and (26), (28) with respect to μ and E . And since the series (23) are rapidly convergent [54], it suffices to take $s_{max} \simeq 10 - 20$ to provide the required precision of calculations (see Section 5).

The results of such “quasi-exact” analytic calculations with the Dirichlet and Neumann boundary conditions for the ground state and the first excited levels “ $2s$ ” and “ $2p$ ” are shown in Figs. 1-2, whence it follows that for atomic H over plane the behavior of levels turns out to be sufficiently different depending on the type of boundary conditions. Under the Dirichlet condition the atom repels itself from the plane, whereas under the Neumann one the atom will occupy an equilibrium position at some finite distance from the plane (see Fig.1). The latter effect is quite understandable, since the Dirichlet condition appears in the limit $\lambda \rightarrow +\infty$, i.e. when the atom reflects from the plane with the maximal force, whereas the Neumann one corresponds to the case of the neutral boundary $\lambda = 0$. At the same time, in both cases with increasing h the ground state levels tend exponentially fast to their common asymptotics, corresponding to that of the free H. Here it would be worthwhile to emphasize that in the considered picture the medium, filling the half-space $z < 0$, is modeled by the boundary condition (4), which represents the summary of all the excitations in the bulk and on its surface and so can be either attractive or repulsive. Therefore, there is every reason for the resulting asymptotics of levels to be significantly different from the attractive van der Waals potential $V_A(h)$, which should fall off asymptotically as $\sim 1/h^6$, and all the more from various corrections like the Casimir-Polder force [55].

Another picture appears for $h \rightarrow 0$. For the Dirichlet condition the electronic WF of atomic H, which nucleus resides directly on the boundary surface $z = 0$, should be odd with respect to reflection in the plane and so admits only those nlm -atomic levels, for which $l+m$ are odd. In

the case of the Neumann condition WF should be even under reflection, hence, the values of $l+m$ should be even too. Therefore by transition from $h \rightarrow \infty$ to $h \rightarrow 0$ the $1s$ -level transforms into $2p$ with $m = 0$ for the Dirichlet condition and into $1s$ for the Neumann one. Remark that during this transition the third quantum number remains unchanged, since l_z is conserved.

A similar picture takes place also for the excited levels “ $2s$ ” and “ $2p$ ” (see Fig.2). In particular, in the case of Dirichlet condition the calculations show that by transition from $h \rightarrow \infty$ to $h \rightarrow 0$ they don’t intersect. Therefore each level corresponds to its “unique” local extremum of the energy functional, fixed in relation to others. It follows whence that during such transition the level $2s$ should transform into $3p$ with $m = 0$, which is the next allowed for $h \rightarrow 0$ after $2p$ with $m = 0$, which in turn is the result of $1s$ -transmutation. At the same time, the level $2p$ with $m = 0$ of the free atom for $h \rightarrow \infty$, being allowed for $h \rightarrow 0$ too, actually rises even higher up to $4f$ with $m = 0$. Here the repulsive property of the Dirichlet boundary condition shows up very clearly. Finally, the level $2p$ with $m = \pm 1$ for $h \rightarrow \infty$ transforms into allowed for $h \rightarrow 0$ level $3d$ with $m = \pm 1$. Such a specific splitting of the first excited ($n = 2$) energy level of free H by transition from $h \rightarrow \infty$ to $h \rightarrow 0$ is closely related to the spherical symmetry breakdown in the problem considered. In the case of $\mathbb{R}^3/2$ with plane boundary there remains instead of the spherical symmetry only the axial one, hence, for finite h the orbital moment isn’t conserved any more, there remains only its projection l_z . As a result, for finite h the electronic WF is a superposition of a large amount of spherical harmonics with their specific radial components, whose analytic form can be found only in the partial cases considered above.

In the Neumann case all the lowest excited levels “ $2s$ ” and “ $2p$ ” with $m = 0, m = \pm 1$ intersect each other, that

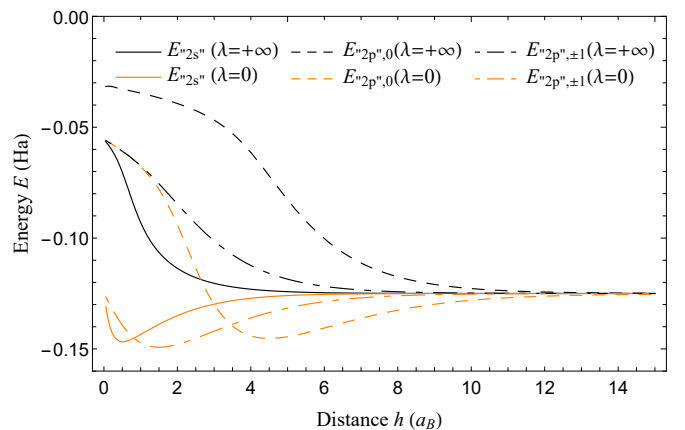


FIG. 2: (Color online). Atomic H energy $E(h)$ of two first excited levels “ $2s$ ” and “ $2p$ ”. For $h \gg a_B$ the solid curves tend to $2s$ -level of the free atom, the dashed ones – to $2p, m = 0$, while the dash-dotted ones – to $2p, m = \pm 1$, respectively, with the common asymptotics of the bound energy, corresponding to $n = 2$ of the free H. Black curves correspond to the Dirichlet condition, while the orange curves – to the Neumann one.

follows directly both from the results of “quasi-exact” analytic solution (26), (28), shown in Fig.2, and from the variational estimates based on the special type trial functions, which are explored below in Sect.4. In this case by transition from $h \rightarrow \infty$ to $h \rightarrow 0$ the level $2s$ transforms into $2s$, $2p$ with $m = 0$ – into $3d$ with $m = 0$, $2p$ with $m = \pm 1$ – into $2p$ with $m = \pm 1$, and every-time the energy minimum takes place for some finite but non-zero h . The latter circumstance reflects the fact that under Neumann condition the direct interaction between the atomic electron and the boundary is actually absent, while the boundary condition itself provides only the electron’s “not going through” property into the forbidden region $z < 0$. Therefore it turns out energetically favorable for the atom to be in the mode of “soaring” over the boundary plane at some finite height.

4. VARIATIONAL ESTIMATES FOR THE LOWEST LEVELS OF ATOMIC H OVER PLANE WITH $\lambda \gtrsim -0.3$

Now – having dealt with the exactly solvable cases this way – let us turn to a more general situation, when the electronic WF on the plane is subject of Robin condition (4) with $\lambda(\vec{\rho}) = \text{const} \neq 0, 1, \infty$. In this case the analytic solution of SE is absent, and so the variational estimates and numerical tools come into play.

As it was shown in the preceding Section, for $\lambda \geq 1$ the mutual reflection between H and plane should be so strong, that the minimal energy is reached only in the case of infinite separation between them. At the same time, for $\lambda < 1$ the effective atomic potential becomes attractive, hence, the minimal energy of the ground state can be reached at finite distances from the boundary surface. This picture is confirmed both via direct numerical calculations (whose detailed description is presented in the next Section 5) and by means of variational estimates with special type electronic trial WF.

In this Section we consider the variational estimates, based on a special modification of the effective charge approximation, which works for $\lambda \gtrsim -0.3$. Since the problem is axially symmetric, we’ll use the cylindric co-ordinate frame (ρ, φ, z) , in which the nucleus is placed at the point $(0, 0, h)$. The exact solution for energy levels corresponds to the local extremes of the functional

$$E[\psi] = \frac{1}{N} \left[\int_{z \geq 0} dz \rho d\rho \left(\frac{1}{2} |\vec{\nabla} \psi|^2 - \frac{|\psi|^2}{\sqrt{\rho^2 + (z-h)^2}} \right) + \frac{\lambda}{2} \int_{z=0} \rho d\rho |\psi|^2 \right], \quad (29)$$

$$N = \int_{z \geq 0} dz \rho d\rho |\psi|^2. \quad (30)$$

The choice of trial functions is based mainly on the following argument. For such values of λ in presence of the

plane the behavior of the electronic WF in the vicinity of the nucleus cannot significantly change, especially for sufficiently large separation between the nucleus and plane. The main effect of interaction between the atomic electron and the border reduces in this case to the screening of the nucleus charge. Therefore it is natural to employ as a first approximation the exact WF of the Coulomb problem in the unbounded space, modified by an effective nucleus charge $q = 2\alpha$ combined with a correction of its behavior near the plane $z = 0$, where the boundary condition (4) should hold. Such a correction can be quite effectively implemented by a multiplier, which changes the logarithmic derivative of WF with respect to z -coordinate. The most suitable version of such a multiplier turns out to be $\exp(-\beta z)$. From one side, inserting this factor enlarges the amount of analytic calculations for the mean energy, but from the other, it remarkably improves the agreement with results of direct numerical calculations.

With account for these considerations the trial ground state WF will be taken in the form of $1s$ -hydrogen function with an effective nucleus charge $q = 2\alpha$ and the additional multiplier $\exp(-\beta z)$, while for the first excited states with $m = \pm 1$ – $2p$ -hydrogen functions with $m = \pm 1$ and the same $q = 2\alpha$ and additional multiplier (the choice of trial WF for the first excited states “ $2s$ ” and “ $2p$ ” with $m = 0$ is discussed below)

$$\psi_{“1s”}^{tr} = \exp(-2\alpha\sqrt{\rho^2 + (z-h)^2} - \beta z), \quad (31)$$

$$\psi_{“2p”, \pm 1}^{tr} = \rho \exp(-\alpha\sqrt{\rho^2 + (z-h)^2} - \beta z \pm i\varphi). \quad (32)$$

The appearance of the factor ρ in $\psi_{“2p”, \pm 1}^{tr}$ is caused by the fact that the complete $2p$ -hydrogen WF with $m = \pm 1$ possesses the angular part, containing $P_1^{\pm 1}(\cos \theta) = \pm \sin \theta$, and so the factor r in the radial part of $2p$ -hydrogen function transforms into ρ .

As a result, upon substituting (31) into (29) we obtain the following expression for the mean value of the ground state energy

$$E_{“1s”}^{tr} = \frac{A_0 + (A_1 + \lambda A_2) \exp[-2h(2\alpha + \beta)]}{A_3 + A_4 \exp[-2h(2\alpha + \beta)]}, \quad (33)$$

with the coefficients in the nominator being equal to

$$\begin{aligned} A_0 &= 32\alpha^2 \frac{\alpha - 1}{8\alpha^2 - 2\beta^2}, \\ A_1 &= -\frac{\beta}{2} - \frac{4\alpha(\alpha - 1)}{2\alpha + \beta} - 2h\alpha(2\alpha + \beta), \\ A_2 &= 1 + 2h\alpha, \end{aligned} \quad (34)$$

while in the denominator

$$A_3 = \frac{32\alpha^3}{(4\alpha^2 - \beta^2)^2}, \quad A_4 = \frac{-\beta - 4\alpha(1 + h(2\alpha + \beta))}{(2\alpha + \beta)^2}. \quad (35)$$

For the first excited “ $2p$ ”-state with $m = \pm 1$ the mean value upon substituting (32) into (29) takes the form

$$E_{“2p”, \pm 1}^{tr} = \frac{B_0 + (B_1 + \lambda B_2) \exp[-2h(2\alpha + \beta)]}{B_3 + B_4 \exp[-2h(2\alpha + \beta)]}, \quad (36)$$

with coefficients

$$\begin{aligned}
B_0 &= \frac{\alpha - 1}{2(\alpha - \beta)^2(\alpha + \beta)^2}, \\
B_1 &= -\left(-8\alpha^2 + 8\alpha^3 - 4\alpha\beta + 7\alpha^2\beta + \right. \\
&\quad \left. + 6\alpha\beta^2 + 3\beta^3 + 4h^2\alpha^2(\alpha + \beta)^3 + 2h\alpha(\alpha + \beta)(5\alpha^2 + \right. \\
&\quad \left. + 4\alpha(-1 + \beta) + 3\beta^2)\right) / \left(32\alpha^4(\alpha + \beta)^2\right), \\
B_2 &= \frac{3 + 6h\alpha + 4h^2\alpha^2}{16\alpha^4},
\end{aligned} \tag{37}$$

and

$$\begin{aligned}
B_3 &= \frac{\alpha}{(\alpha^2 - \beta^2)^3}, \\
B_4 &= -\left(2\alpha^2(4 + h\alpha(5 + 2h\alpha)) + \alpha(9 + 8h\alpha(2 + h\alpha))\beta + \right. \\
&\quad \left. + (3 + 2h\alpha(3 + 2h\alpha))\beta^2\right) / \left(16\alpha^4(\alpha + \beta)^3\right).
\end{aligned} \tag{38}$$

Here it should be noted that the condition of orthogonality to the ground state for the trial functions of excited levels is exactly fulfilled only for the trial WF (32) with $m = \pm 1$. In the trial WF for excited levels with $m = 0$ there might exist an admixture of the exact ground state WF. Therefore the variational estimate for the ground state majorizes always its exact energy from above, the same should take place for the first excited state with $m = \pm 1$, whereas for the excited states with $m = 0$ in the general case this statement might be incorrect.

So for two remaining first excited states “2s” and “2p” with $m = 0$ the choice of the trial functions turns out to be more complicated. First, there follows from the analytic solution in the Neumann case (see Sect.3) that in presence of the boundary plane such states undergo hybridization. In this case the natural choice for trial functions is their linear combination

$$\psi_{\text{exact},m=0}^{\text{tr}} = \psi_{\text{“2s”}}^{\text{tr}} \cos(\chi) + \psi_{\text{“2p”},0}^{\text{tr}} \sin(\chi), \tag{39}$$

where χ is the mixture variational parameter,

$$\psi_{\text{“2s”}}^{\text{tr}} = (\sqrt{\rho^2 + (z - h)^2} - \gamma) \exp(-\alpha\sqrt{\rho^2 + (z - h)^2} - \beta z), \tag{40}$$

$$\psi_{\text{“2p”},0}^{\text{tr}} = (z - h) \exp(-\alpha\sqrt{\rho^2 + (z - h)^2} - \beta z). \tag{41}$$

The multiplier $(z - h)$ in $\psi_{\text{“2p”},0}^{\text{tr}}$ is caused by the same reason as ρ in $\psi_{\text{“2p”},\pm 1}^{\text{tr}}$.

The parameter γ , which enters the expression (40) for $\psi_{\text{“2s”}}^{\text{tr}}$, is determined from the condition of orthogonality between $\psi_{\text{exact},m=0}^{\text{tr}}$ and the trial ground state function $\psi_{\text{“1s”}}^{\text{tr}}$ (31)

$$\int_{z \geq 0} dz \rho d\rho \psi_{\text{“1s”}}^{\text{tr}} \psi_{\text{exact},m=0}^{\text{tr}} = 0, \tag{42}$$

in order to reduce, if possible, the admixture of the ground state WF (but not to remove completely!). The explicit answer for γ reads

$$\begin{aligned}
\gamma &= \\
&= \frac{C_0}{(9\alpha^2 - 4\beta^2)^3} + \frac{\exp[-3h\alpha - 2h\beta]}{(27\alpha^3(3\alpha + 2\beta)^3)} (C_1 \sin(\chi) + C_2 \cos(\chi)) \\
&\quad \frac{C_3}{(9\alpha^2 - 4\beta^2)^2} + \frac{\exp[-3h\alpha - 2h\beta]}{9\alpha^2(3\alpha + 2\beta)^2} C_4 \cos(\chi)
\end{aligned} \tag{43}$$

where the coefficients in the nominator are equal to

$$\begin{aligned}
C_0 &= -4\left((27\alpha^2 + 4\beta^2) \cos(\chi) - 24\alpha\beta \sin(\chi)\right), \\
C_1 &= 3\alpha\left(9\alpha + 27h\alpha^2 + 27h^2\alpha^3 + 2\beta + 24h\alpha\beta + \right. \\
&\quad \left. + 36h^2\alpha^2\beta + 4h\beta^2 + 12h^2\alpha\beta^2\right), \\
C_2 &= 54\alpha^2 + 108h\alpha^3 + 81h^2\alpha^4 + 36\alpha\beta + 108h\alpha^2\beta + \\
&\quad + 108h^2\alpha^3\beta + 8\beta^2 + 24h\alpha\beta^2 + 36h^2\alpha^2\beta^2,
\end{aligned} \tag{44}$$

while in the denominator

$$C_3 = -12\alpha \cos(\chi), \quad C_4 = 6\alpha + 9h\alpha^2 + 2\beta + 6h\alpha\beta. \tag{45}$$

Upon substituting the representation (39) for $\psi_{\text{exact},m=0}^{\text{tr}}$ into (29) the mean value of energy for these levels takes the form

$$E_{\text{exact},m=0}^{\text{tr}} = \frac{N_0 + (N_1 + \lambda N_2) \exp[-2h(\alpha + \beta)]}{N_3 + N_4 \exp[-2h(\alpha + \beta)]}. \tag{46}$$

The coefficients N_i in eq.(46) have the following structure

$$N_i = \frac{a_i + b_i \sin(2\chi) + c_i \cos(2\chi)}{d_i}, \tag{47}$$

where

$$\begin{cases} a_0 = -4\alpha^2 + 2\alpha^3 - 4\beta^2 + 2\alpha\beta^2 + 4\alpha^3\gamma - \alpha^4\gamma - 4\alpha\beta^2\gamma + \beta^4\gamma - 2\alpha^4\gamma^2 + \alpha^5\gamma^2 + \\ + 4\alpha^2\beta^2\gamma^2 - 2\alpha^3\beta^2\gamma^2 - 2\beta^4\gamma^2 + \alpha\beta^4\gamma^2, \\ b_0 = 2(\alpha - 2)\beta(\alpha^2\gamma - \beta^2\gamma - 2\alpha), \\ c_0 = (\alpha^2 - \beta^2)(\alpha^3\gamma^2 + \beta^2\gamma(2\gamma - 1) - \alpha^2\gamma(1 + 2\gamma) + \alpha\gamma(4 - \beta^2\gamma) - 2), \\ d_0 = 8(\alpha^2 - \beta^2)^3, \end{cases} \tag{48}$$

$$\left\{ \begin{array}{l}
a_1 = -16\alpha^3 + 8\alpha^4 - 24h\alpha^4 + 10h\alpha^5 - 16h^2\alpha^5 + 4h^2\alpha^6 + 8h^3\alpha^7 - 12\alpha^2\beta + 9\alpha^3\beta - \\
- 32h\alpha^3\beta + 16h\alpha^4\beta - 32h^2\alpha^4\beta + 12h^2\alpha^5\beta + 32h^3\alpha^6\beta - 4\alpha\beta^2 + 11\alpha^2\beta^2 - 8h\alpha^2\beta^2 + \\
+ 16h\alpha^3\beta^2 - 16h^2\alpha^3\beta^2 + 20h^2\alpha^4\beta^2 + 48h^3\alpha^5\beta^2 + 9\alpha\beta^3 + 16h\alpha^2\beta^3 + 20h^2\alpha^3\beta^3 + \\
+ 32h^3\alpha^4\beta^3 + 3\beta^4 + 6h\alpha\beta^4 + 8h^2\alpha^2\beta^4 + 8h^3\alpha^3\beta^4 + 16\alpha^4\gamma - 4\alpha^5\gamma + 16h\alpha^5\gamma - \\
- 8h\alpha^6\gamma - 8h^2\alpha^7\gamma + 24\alpha^3\beta\gamma - 8\alpha^4\beta\gamma + 32h\alpha^4\beta\gamma - 24h\alpha^5\beta\gamma - 32h^2\alpha^6\beta\gamma + \\
+ 8\alpha^2\beta^2\gamma - 12\alpha^3\beta^2\gamma + 16h\alpha^3\beta^2\gamma - 32h\alpha^4\beta^2\gamma - 48h^2\alpha^5\beta^2\gamma - 12\alpha^2\beta^3\gamma - \\
- 24h\alpha^3\beta^3\gamma - 32h^2\alpha^4\beta^3\gamma - 4\alpha\beta^4\gamma - 8h\alpha^2\beta^4\gamma - 8h^2\alpha^3\beta^4\gamma - 8\alpha^5\gamma^2 + 4\alpha^6\gamma^2 + \\
+ 4h\alpha^7\gamma^2 - 16\alpha^4\beta\gamma^2 + 10\alpha^5\beta\gamma^2 + 16h\alpha^6\beta\gamma^2 - 8\alpha^3\beta^2\gamma^2 + 10\alpha^4\beta^2\gamma^2 + 24h\alpha^5\beta^2\gamma^2 + \\
+ 6\alpha^3\beta^3\gamma^2 + 16h\alpha^4\beta^3\gamma^2 + 2\alpha^2\beta^4\gamma^2 + 4h\alpha^3\beta^4\gamma^2 , \\
b_1 = 2\alpha(\beta^3(2h\beta - 1) + 4h^2\alpha^6(h - \gamma) + 2h\alpha^5(1 + 8h\beta)(h - \gamma) + \alpha\beta(2h\beta^3(2h - \gamma) + \\
+ \beta^2(4h + \gamma) - 2 - (3 + 4h)\beta) + \alpha^4(24h^3\beta^2 - \gamma + h(4 - 4(\beta - 2)\gamma) + \\
+ h^2(6\beta - 24\beta^2\gamma - 8)) + \alpha^3(2 + 16h^3\beta^3 + (4 + \beta)\gamma - 2h^2\beta(8 - 5\beta + 8\beta^2\gamma) - \\
- 4h(3 + \beta^2\gamma - \beta(1 + 4\gamma))) + \alpha^2(2h\beta^3(5h - 2\gamma) - 2\beta(1 + 8h - 2\gamma) + \\
+ 4h^2\beta^4(h - \gamma) + \beta^2(-8h^2 + 3\gamma + h(2 + 8\gamma)) - 6) , \\
c_1 = -(\alpha + \beta)(-3\beta^3 + 4h\alpha^6(2h - \gamma)\gamma + 2\alpha\beta(2 - 3\beta + \beta^2(2\gamma - 3h)) - \\
- 4\alpha^5(\gamma^2 + h^2(1 - 6\beta\gamma) + h\gamma(3\beta\gamma - 2)) + \alpha^2(8 + \beta(8h - 8\gamma - 3) + \\
+ \beta^2(8\gamma - 14h) - 2\beta^3(2h^2 - 4h\gamma + \gamma^2)) + 2\alpha^4(\gamma(2 + 4\gamma - 3\beta\gamma) + 6h^2\beta(2\beta\gamma - 1) - \\
- h(1 + 8\gamma - 8\beta\gamma + 6\beta^2\gamma^2)) + 2\alpha^3(2h^2\beta^2(2\beta\gamma - 3) + 2\gamma(\beta + 2\beta\gamma - \beta^2\gamma - 4) + \\
+ h(4 - 5\beta - 8\beta\gamma + 8\beta^2\gamma - 2\beta^3\gamma^2)) , \\
d_1 = -64\alpha^4(\alpha + \beta)^3 ,
\end{array} \right. \quad (49)$$

$$\left\{ \begin{array}{l}
a_2 = \frac{3}{2} + 3h\alpha + 4h^2\alpha^2 + 4h^3\alpha^3 - 2\alpha\gamma - 4h\alpha^2\gamma - 4h^2\alpha^3\gamma + \alpha^2\gamma^2 + 2h\alpha^3\gamma^2 , \\
b_2 = 2h\alpha(1 + \alpha(2h - \gamma) + 2\alpha^2(h^2 - h\gamma)) , \\
c_2 = \frac{3}{2} + 3h\alpha + 2h^2\alpha^2 - 2\alpha\gamma - 4h\alpha^2\gamma - 4h^2\alpha^3\gamma + \alpha^2\gamma^2 + 2h\alpha^3\gamma^2 , \\
d_2 = 8\alpha^4 ,
\end{array} \right. \quad (50)$$

$$\left\{ \begin{array}{l}
a_3 = 4\alpha^3 + 8\alpha\beta^2 - 3\alpha^4\gamma + 2\alpha^2\beta^2\gamma + \beta^4\gamma + \alpha^5\gamma^2 - 2\alpha^3\beta^2\gamma^2 + \alpha\beta^4\gamma^2 , \\
b_3 = -2\beta(5\alpha^2 + \beta^2 - 2\alpha^3\gamma + 2\alpha\beta^2\gamma) , \\
c_3 = (\alpha^2 - \beta^2)(\alpha^3\gamma^2 - 3\alpha^2\gamma - \beta^2\gamma + \alpha(2 - \beta^2\gamma^2)) , \\
d_3 = 4(\alpha^2 - \beta^2)^4 ,
\end{array} \right. \quad (51)$$

$$\left\{ \begin{array}{l}
a_4 = 16\alpha^3 + 26h\alpha^4 + 20h^2\alpha^5 + 8h^3\alpha^6 + 19\alpha^2\beta + 46h\alpha^3\beta + 48h^2\alpha^4\beta + 24h^3\alpha^5\beta + \\
+ 12\alpha\beta^2 + 26h\alpha^2\beta^2 + 36h^2\alpha^3\beta^2 + 24h^3\alpha^4\beta^2 + 3\beta^3 + 6h\alpha\beta^3 + 8h^2\alpha^2\beta^3 + 8h^3\alpha^3\beta^3 - \\
- 12\alpha^4\gamma - 16h\alpha^5\gamma - 8h^2\alpha^6\gamma - 24\alpha^3\beta\gamma - 40h\alpha^4\beta\gamma - 24h^2\alpha^5\beta\gamma - 16\alpha^2\beta^2\gamma - \\
- 32h\alpha^3\beta^2\gamma - 24h^2\alpha^4\beta^2\gamma - 4\alpha\beta^3\gamma - 8h\alpha^2\beta^3\gamma - 8h^2\alpha^3\beta^3\gamma + 4\alpha^5\gamma^2 + 4h\alpha^6\gamma^2 + \\
+ 10\alpha^4\beta\gamma^2 + 12h\alpha^5\beta\gamma^2 + 8\alpha^3\beta^2\gamma^2 + 12h\alpha^4\beta^2\gamma^2 + 2\alpha^2\beta^3\gamma^2 + 4h\alpha^3\beta^3\gamma^2 , \\
b_4 = 2\alpha(\beta^2(1 + 2h\beta) + 4h^2\alpha^5(h - \gamma) + \alpha\beta(1 + 2h\beta)(4 + 2h\beta - \beta\gamma) + \\
+ 2h\alpha^4(6h^2\beta - 3\gamma + h(5 - 6\beta\gamma)) + 2\alpha^2(1 + 2h\beta)(3 + h^2\beta^2 - 2\beta\gamma + h\beta(4 - \beta\gamma)) + \\
+ \alpha^3(12h^3\beta^2 - 3\gamma - 12h^2\beta(\beta\gamma - 2) - 2h(7\beta\gamma - 6))) , \\
c_4 = -(\alpha + \beta)(4h\alpha^5(2h - \gamma)\gamma - 3\beta^2 + \alpha\beta(4\beta\gamma - 9 - 6h\beta) - 2\alpha^2(4 + 2h^2\beta^2 - \\
- 6\beta\gamma + \beta^2\gamma^2 - 4h\beta(\beta\gamma - 2)) - 4\alpha^4(\gamma^2 + h^2(1 - 4\beta\gamma) + 2h\gamma(\beta\gamma - 2)) + \\
+ 2\alpha^3(4h^2\beta(\beta\gamma - 1) - 3\gamma(\beta\gamma - 2) + h(12\beta\gamma - 2\beta^2\gamma^2 - 5))) , \\
d_4 = -32\alpha^4(\alpha + \beta)^4 .
\end{array} \right. \quad (52)$$

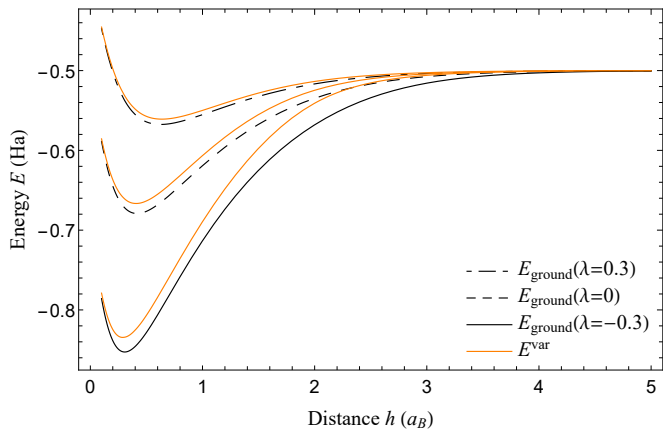


FIG. 3: (Color online). Atomic H ground state energy $E(h)$ as a function of the nucleus position over plane h for the general Robin condition on the boundary plane. Black curves correspond to direct numerical results, while the orange ones – to variational estimates by means of the trial function (31).

For $\lambda \gtrsim -0.3$ the minimization of expressions (33), (36) and (46) with respect to the variational parameters α, β gives a satisfactory agreement with the results of direct numerical calculations, at least on the qualitative level. The dependence of the ground state “1s” and first excited “2p” with $m = \pm 1$ on the nucleus position h , found via such variational estimates, is shown in Figs.3,4 in comparison with the direct numerical results.

Let us remark specially that by means of the trial functions (31), (32) and (39)-(41) there are visible only the levels with exponential asymptotics for $h \gg a_B$, which in this case tend to the corresponding levels of free H with $n = 1$ or $n = 2$. At the same time, the levels with the power-like asymptotics, which appear already for $\lambda = -0.3$ and tend to the limiting point $-\lambda^2/2 = -0.045 Ha$, cannot be caught by means of such substitutions for ψ^{tr} , since their electronic WF possess a substantially different structure.

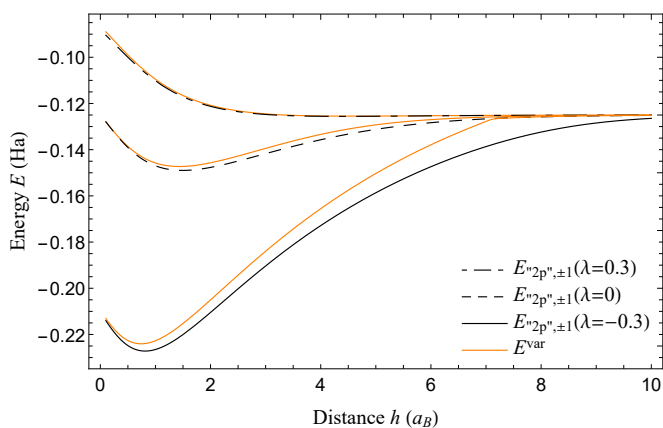


FIG. 4: (Color online). $E(h)$ of the first excited level with $m = \pm 1$, which tend to 2p for $h \gg a_B$, for the general Robin condition on the boundary plane. Black curves correspond to direct numerical results, while the orange ones – to variational estimates by means of the trial function (32).

There follows from Fig.3 that for the considered values of λ and $h \gtrsim 4 a_B$ the ground state energy is practically indistinguishable from the 1s level of free H. On the other hand, with decreasing h the bound energy increases, and the faster, the more negative the value of λ , and hence, the stronger the attraction between the electron and the plane $z = 0$. With decreasing λ there also grows the maximal value of the bound energy, exceeding for $\lambda = 0.3$ the value $0.568 Ha$ at $h_{max} = 0.627 a_B$, for $\lambda = 0$ — $0.679 Ha$ at $h_{max} = 0.417 a_B$, for $\lambda = -0.3$ — $0.853 Ha$ at $h_{max} = 0.307 a_B$. Collected together, all these facts indicate that when the atom approaches the plane, the electronic WF deforms the faster, the greater the attraction between the atom and the boundary plane.

It should be also noted that the difference between the variational estimates and direct calculations increases in the same way. Therefore, the efficiency of the multiplier $\exp(-\beta z)$, deforming the trial function in order to take account of the boundary plane $z = 0$, decreases with varying λ from positive to negative values.

A similar picture one finds in Fig.4, where the dependence on h for the level “2p” with $m = \pm 1$ in the same range of λ is presented. As in the case of the ground state, with increasing h all the curves tend to the corresponding energy $-0.125 Ha$ of 2p-level of free H. However, now the levels closely approach their limiting value much later, at the scale $h \gg 10 a_B$. In addition, Fig.4 confirms explicitly the remark concerning the exact orthogonality between the trial function (32) and the ground state WF, since the variational curves lie everywhere higher than the direct numerical results.

In Figs.5 the results of variational estimates, based on the Ansatz (39)-(41) for the trial function, and numerical calculations for the first two excited levels with $m = 0$ and $\lambda = 0.3, 0, -0.3$, are presented. In this case the levels approach closely their limiting values only at the scales $h \gg 10 a_B$. From Fig.5b there follows also that the trial function (39) permits to reproduce the hybridization of excited levels with $m = 0$, obtained analytically in Sect.3 for $\lambda = 0$. It would be also worth to note that in this case for certain values of λ the variational curves lie below the numerical results, that points at the presence of the ground state WF admixture in the trial functions (39)-(41) and so in the mean value of the energy (46).

Thus, in the considered range of λ the trial WF (31), (32) and (39)-(41) are able to reproduce qualitatively the behavior of corresponding atomic H energy levels, obtained via direct numerical calculations. As expected, the variational estimate reproduces the result the worse, the more negative the value of λ . The reason is simple — for sufficiently negative λ the true electronic WF transforms into a superposition of a large amount of spherical harmonics in the form of a “drop” stuck and partially spread on the border plane, and hence, cannot be described in terms of such simple trial functions.

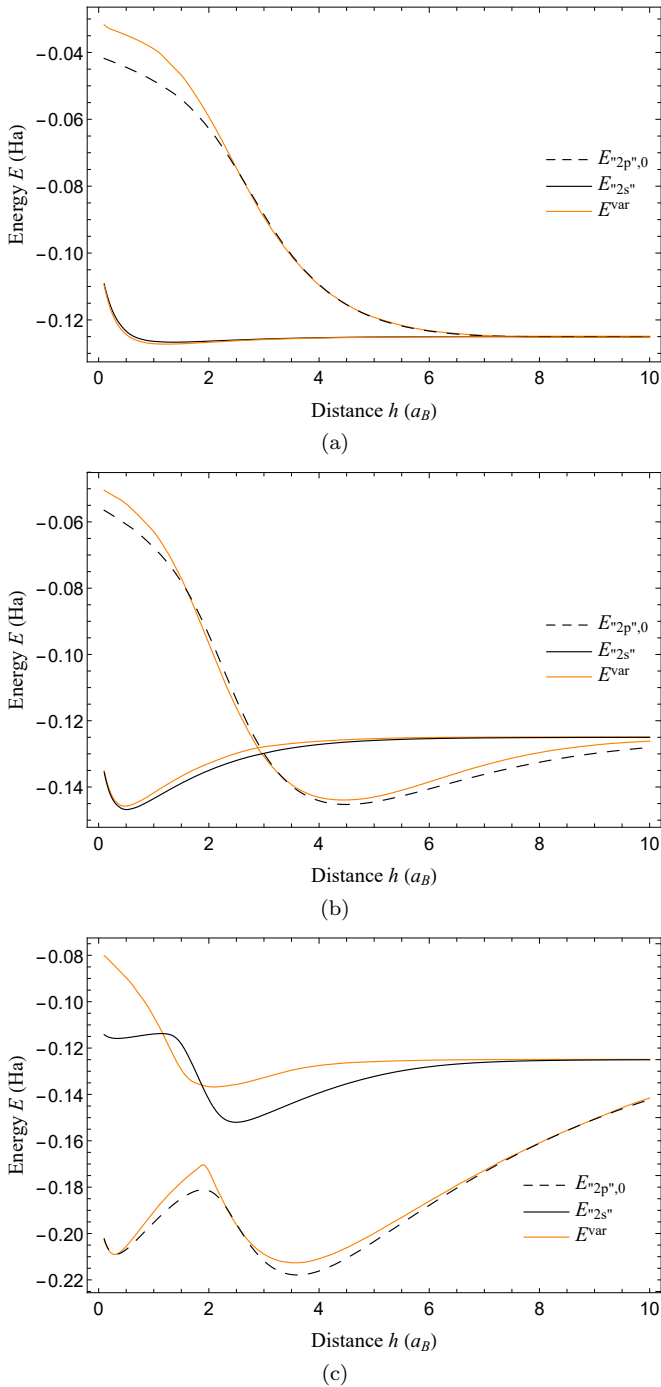


FIG. 5: (Color online). The dependence of two first excited levels with $m = 0$ on h for (a): $\lambda = 0.3$; (b) $\lambda = 0$; (c) $\lambda = -0.3$. Black curves correspond to direct numerical results, while the orange ones – to variational estimates by means of the trial function (39)-(41).

5. ATOMIC H OVER PLANE IN THE GENERAL CASE: DIRECT NUMERICAL CALCULATIONS AND VARIATIONAL ESTIMATES FOR THE LOWEST LEVELS

For atomic H in $\mathfrak{R}^3/2$ the most efficient numerical tool is the pertinent modification of the finite element method [56] within the direct variational approach to the functional (29), considered on a spatial lattice as a function of variables $\psi_{ij} = \psi(\rho_i, z_j)$. The calculations have been performed for the ground state and two first excited states in the range $-1.2 \leq \lambda \leq 0.3$ and $0.2 a_B \leq h \leq 10 a_B$. As the effective spatial infinity for the numerical problem $z_{max} = \rho_{max} = 40 a_B$ is chosen. The results of performed calculations confirm that such a choice is quite satisfactory, since its further enlarging doesn't yield any appreciable changes within the precision achieved. In particular, for the ground state and $h \simeq 10 a_B$ the relative error between the numerical and variational calculations grows up with decreasing λ , but doesn't exceed $\simeq 1.5 \times 10^{-3}$. For the excited states in the considered range of λ the relative error is $\sim 10^{-2}$. Therefore the behavior of the lowest levels for $h \gtrsim 10 a_B$ can be obtained without employing cumbersome lattice calculations, just by means of variational estimates, considered below.

Within this method the integrals in the functional (29) are replaced by the integral sums according to trapezoid approximation, afterwards the extremes of the function of lattice variables $\psi_{ij} = \psi(\rho_i, z_j)$ are sought. In the case of excited states the condition of orthogonality of corresponding solutions to the ground state WF is added. The precision of calculations is controlled via changing the lattice step, that allows for additional increase of the accuracy of calculations by extrapolating the dependence of the obtained results on the magnitude of the square of the lattice spacing to its value tending to zero. In concrete calculations there have been used four subsequent lattices, the number of nodes in which (per both coordinates) is related as 1:2:3:4. The relative error, obtained by comparison the extrapolation result for three first lattices with the result of extrapolation for four lattices, is $O(10^{-4})$ for the ground state and $O(10^{-3})$ for the excited states.

Furthermore, the direct numerical analysis allows to trace how the levels tend to their asymptotic values for $h \rightarrow \infty$, since for $\lambda < 0$ the levels reveal two types of asymptotical behavior. If the electron-nucleus interaction is stronger than the electron-plane one, then for $h \gg a_B$ the electron resides mostly in the vicinity of the nucleus, while its bound energy tends to the corresponding level of the free H exponentially fast according to (15).

To the contrary, in the case of dominating interaction with plane the lowest electronic states correspond to the picture, wherein the electron leaves the nucleus and resides mostly in the vicinity of the plane, while the asymptotics of these levels with increasing h is a power-like one similar to (14) with the common limiting point $(-\lambda^2/2)$. Quite similar to the case of an atom in the center of a

large spherical cavity [30, 31], this effect becomes more pronounced the more negative λ . It should be remarked, however, that in contrast to the case of a spherical cavity with $R \rightarrow \infty$, when the orbital moment is conserved and the power levels possess the quantum numbers lm , in the presence of boundary plane even for $h \rightarrow \infty$ there remains only l_z as a conserved quantity, and hence, these power-like levels can no longer be classified by the values of the orbital moment.

In the case under consideration for the ground state and the first excited levels one has two critical values of the coupling constant $\lambda_{crit,1} = -1$ and $\lambda_{crit,2} = -1/2$, respectively. In the case when $\lambda > \lambda_{crit,2}$, the asymptotics of the ground state and the first excited ones coincides with the lowest levels $1s$, $2s$ and $2p$ of free H with energies $-1/2$ and $-1/8$, correspondingly, and this asymptotics is reached exponentially fast in the way similar to the law (15). When $\lambda = \lambda_{crit,2}$, the ground state asymptotics for $h \rightarrow \infty$ is still exponential and corresponds to $1s$ -level of free H, but the first excited ones transform into the second type of levels with power-like asymptotics and the common limiting point $-\lambda_{crit,2}^2/2 = -1/8$, still coinciding with the energy level with $n = 2$ of free H. Moreover, as it was already mentioned in Sect.2 (see formulae (18),(19)), in this case due to von Neumann-Wigner avoided crossing effect the power-like levels approach their limiting point $-1/8$ from below, whereas the exponential ones, corresponding to $2s$ and $2p$ levels of free H, from above. When $\lambda_{crit,2} > \lambda > \lambda_{crit,1}$, the asymptotics of the ground state and of the first excited levels is $-1/2$ and $-1/2 < -\lambda^2/2 < -1/8$, respectively, but the latter one is achieved remarkably slower, following a power law. In the case $\lambda = \lambda_{crit,1}$ there works once more the avoided crossing effect. Namely, the lowest level and a finite number of first excited reveal now the power-like behavior with the common limiting value equal to E_{1s} , while the exponential one becomes the next excited level and approaches the same asymptotics from above. For details see Refs.[30], Figs.7,8 and [31], Fig.5. The only difference here is that in Refs.[30, 31] the nucleus is placed in the center of cavity and so both quantum numbers lm serve as a superselection rule, whereas in the present case we have to deal outright with a whole bundle of power-like excited levels without any definite value of the orbital moment. For $\lambda < \lambda_{crit,1}$ the ground state together with the first excited levels tend to their common limiting point $-\lambda^2/2 < -1/2$ according to the power law, while all the others with growing h approach exponentially fast the levels of free H. In this case we meet again the situation, when the exponential level, corresponding in the asymptotics to the $1s$ state of free H, becomes the first of the excited ones with exponential asymptotics, but not the first between all the excited levels, since there will be a set of the first power-like excited levels, which lie below E_{1s} . It should be also noted that for $\lambda \leq \lambda_{crit,1}$ the atomic ground state represents a configuration, in which due to the strong attraction to the border its electronic WF is located almost completely in the vicinity of the latter with a small pick at the nucleus

position, while the energy approaches its asymptotics for $h \rightarrow \infty$ much slower, actually following the hyperbolic law.

As it was already mentioned in Sect.4, the trial functions (31),(32) and (39)-(41), supplied with the effective nucleus charge and modulation of their behavior in the plane vicinity through the multiplier $\exp(-\beta z)$, cannot serve as the base for the estimates of power-like levels. For the approximate description of the latter some more complicated superpositions of hydrogen functions, modulated by the factors similar to $\exp(-\beta z)$ for an effective account of the boundary plane, are needed. For the first three levels with $m = 0$ it suffices to take into account only these multipliers, provided the linear combination of the first 6 hydrogen functions is employed and the same argument as before in Sect.4 is used: the behavior of the electronic WF in the nucleus vicinity cannot be strongly distorted in presence of the plane, especially for sufficiently large distances between the nucleus and plane.

Proceeding further this way, let us use as trial functions for three first states with $m = 0$ the following superpositions

$$\psi^{tr} = \sum_{i=1}^6 c_i \psi_i^{tr} , \quad (53)$$

with ψ_i^{tr} being the WF of first 6 hydrogen levels $1s, 2s, 2p, 3s, 3p, 3d$ with $l_z = 0$, modulated by the factors $\exp(-\beta_i z)$

$$\begin{aligned} \psi_1^{tr} &= \exp(-\sqrt{\rho^2 + (z-h)^2} - \beta_1 z) , \\ \psi_2^{tr} &= (\sqrt{\rho^2 + (z-h)^2} - 2) \exp(-\frac{1}{2}\sqrt{\rho^2 + (z-h)^2} - \beta_2 z) , \\ \psi_3^{tr} &= (z-h) \exp(-\frac{1}{2}\sqrt{\rho^2 + (z-h)^2} - \beta_3 z) , \\ \psi_4^{tr} &= \left(2[\rho^2 + (z-h)^2] - 18\sqrt{\rho^2 + (z-h)^2} + 27 \right) \times \\ &\quad \times \exp(-\frac{1}{3}\sqrt{\rho^2 + (z-h)^2} - \beta_4 z) , \\ \psi_5^{tr} &= (z-h) \left(\sqrt{\rho^2 + (z-h)^2} - 6 \right) \times \\ &\quad \times \exp(-\frac{1}{3}\sqrt{\rho^2 + (z-h)^2} - \beta_5 z) , \\ \psi_6^{tr} &= (\rho^2 - 2(z-h)^2) \exp(-\frac{1}{3}\sqrt{\rho^2 + (z-h)^2} - \beta_6 z) . \end{aligned} \quad (54)$$

The variational estimate is implemented via the energy functional minimization with respect to variational parameters $\vec{\beta} = \{\beta_i\}_{i=1}^6$ and $\vec{c} = \{c_i\}_{i=1}^6$. The energy functional takes the form

$$E^{tr}[\vec{\beta}, \vec{c}] = \frac{\langle \vec{c} | A(\vec{\beta}) | \vec{c} \rangle}{\langle \vec{c} | B(\vec{\beta}) | \vec{c} \rangle} , \quad (55)$$

where the matrices $A(\vec{\beta})$ and $B(\vec{\beta})$ are determined as

follows

$$A_{ij}(\vec{\beta}) = \int_{z \geq 0} dz \rho d\rho \left[\frac{1}{2} (\vec{\nabla} \psi_i^{tr}) (\vec{\nabla} \psi_j^{tr}) - \frac{\psi_i^{tr} \psi_j^{tr}}{\sqrt{\rho^2 + (z-h)^2}} \right] + \frac{\lambda}{2} \int_{z=0} \rho d\rho \psi_i^{tr} \psi_j^{tr}, \quad (56)$$

$$B_{ij}(\vec{\beta}) = \int_{z \geq 0} dz \rho d\rho \psi_i^{tr} \psi_j^{tr}. \quad (57)$$

In the next step we diagonalize the matrix $\langle \vec{c} | B | \vec{c} \rangle$ by finding the eigenvalues b_i and eigenvectors $|\sigma_i\rangle$ of the matrix B with subsequent replacement

$$|\vec{c}\rangle = B^{-1/2} |\vec{\chi}\rangle, \quad (58)$$

where

$$B^{-1/2} = \sum_i \frac{1}{\sqrt{b_i}} |\sigma_i\rangle \langle \sigma_i|. \quad (59)$$

As a result, the minimization of the functional (55) reduces to finding eigenvalues of the matrix \tilde{A}

$$\det [\tilde{A}(\vec{\beta}) - a(\vec{\beta}) E] = 0, \quad (60)$$

where

$$\tilde{A}(\vec{\beta}) = B^{-1/2} A B^{-1/2} = \sum_{ij} |\sigma_i\rangle \frac{\langle \sigma_i | A | \sigma_j \rangle}{\sqrt{b_i b_j}} \langle \sigma_j|. \quad (61)$$

The minima of found this way eigenvalues $a_i(\vec{\beta})$ with respect to variational parameters $\vec{\beta}$ present the variational estimates for the energy levels, corresponding to linear combinations of the form (53).

The results of calculations based on (60),(61) in comparison with the direct numerical analysis and exact answers in corresponding partial cases are presented in Figs.6-9. In Figs.6,7 the variational estimates based on (60),(61) and the results of direct numerical calculations in comparison with the analytic answers for the ground state energy and two first excited levels, found from (26), (28), are shown in dependence on h for the Neumann case with $\lambda = 0$. From Fig.7 it should be clearly seen that the trial functions of excited levels with $m = 0$, constructed as linear combinations (53),(54), are exactly orthogonal to the ground state WF, since in Fig.7 the corresponding variational curves of excited levels lie always higher than the numerical and exact analytic ones.

In Fig.8 the ground state level is shown for $\lambda = 0.3, 0, -0.3, -0.6, -0.9, -1.2$ in dependence on the distance h . There follows from Fig.8 that for $-0.9 \leq \lambda \leq +0.3$ the asymptotics of the ground state for $h \rightarrow \infty$ is exponential and tends to the "normal" 1s-level of

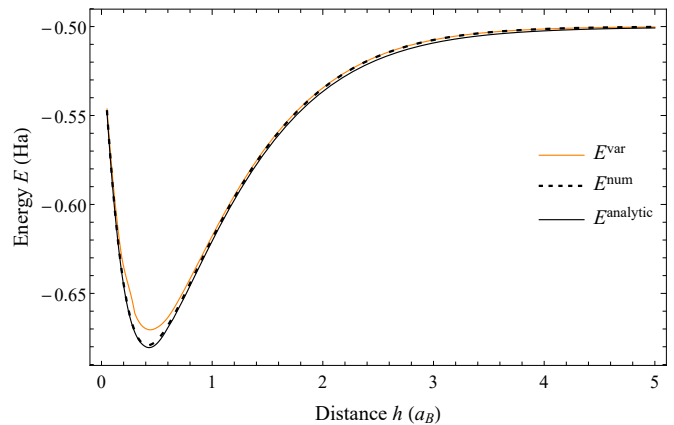


FIG. 6: (Color online). Variational estimate based on (60),(61), the result of direct numerical calculations in comparison with the analytic answer for the ground state energy, found from (26), (28), in dependence on h for the Neumann case with $\lambda = 0$.

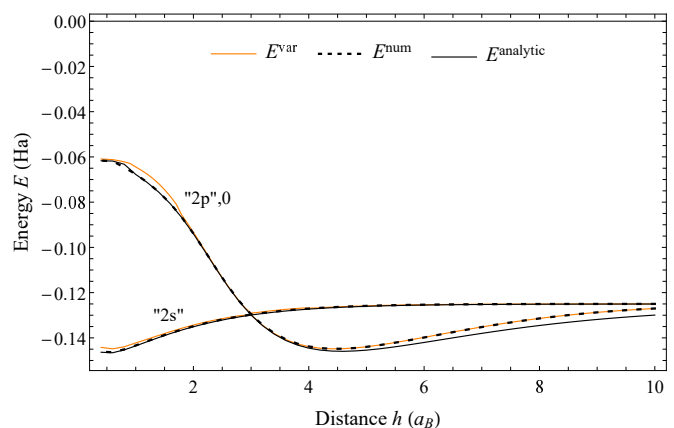


FIG. 7: (Color online). Variational estimates based on (60),(61), the results of direct numerical calculations in comparison with the analytic answers for two first excited levels with $m = 0$, found from (26), (28), in dependence on h for the Neumann case with $\lambda = 0$.

free H with $E_{1s} = -0.5 Ha$, whereas for $\lambda = -1.2$ it represents a power-like one with the limiting energy $-\lambda^2/2 = -0.72 Ha$. It is also clearly seen that in the case of exponential asymptotics for $-0.9 \leq \lambda \leq +0.3$ the ground state levels approach closely the value E_{1s} already for $4 \lesssim h \lesssim 8 a_B$, whereas for $\lambda = -1.2$ the power-like ground state level lies substantially below its asymptotical value even for $h \simeq 10 a_B$. It should be also mentioned that the minima of all the curves shown in Fig.8 are well-pronounced, but at the same time they lie very close to the border and so are actually indistinguishable against the background of inhomogeneities in atomic layers on the boundary surface (for a more accurate representation of what is meant here see, e.g., Ref.[57], Fig.1.1.)

In Figs.9 the dependence $E(h)$ is shown for two first excited levels with $\lambda = 0.3, -0.3$. The case $\lambda = 0$ for these levels is already presented in Fig.2. There follows

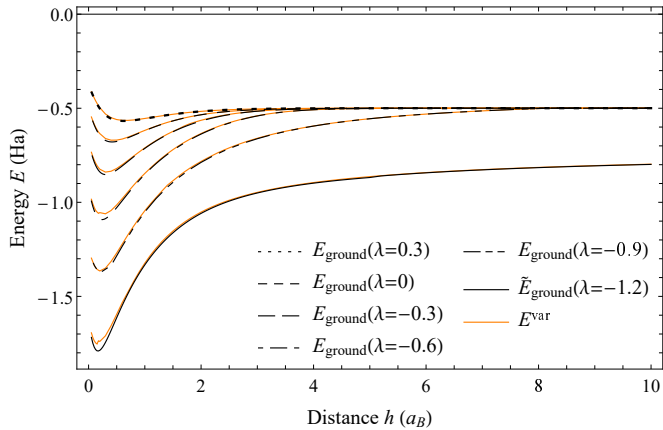


FIG. 8: (Color online). $E(h)$ for the ground state and $\lambda = 0.3, 0, -0.3, -0.6, -0.9, -1.2$. Variational estimates vs the results of direct numerical calculations.

from these drawings that the asymptotics of excited levels for $h \rightarrow \infty$ coincides with those of free H, but if for $\lambda = 0.3$ the levels approach their asymptotical values already for $h \simeq 7 a_B$, in the case of $\lambda = 0$ this situation occurs for $h \simeq 10 a_B$, whereas for $\lambda = -0.3$ it comes out of the considered range of h .

It would be also worth to remark that from Figs.6-9 there follows that the variational estimate is worse reproducing the results of numerical calculations, the more negative the value of λ and the closer the nucleus is to the plane. At the same time, the choice of the trial function in the form (53),(54) permits to reproduce the effect of hybridization of excited levels for $m = 0$ and $\lambda = 0$, which has been detected earlier analytically. Note also that in Figs.6-9 all the variational curves, corresponding to excited levels, lie above the direct numerical results. It isn't, however, the general case, since such a choice of trial functions doesn't provide automatically their orthogonality to the ground state WF and so doesn't prevent the situation, when the variational curves lie below the numerical ones due to admixture of the ground state WF.

In Figs.10 the dependence on h of first four levels with $m = 0$ is shown for $\lambda = -0.9, -1.2$. For such λ the variational estimates, which are quite effective in description of the ground state level even in the power-like case with $\lambda = -1.2$ (see Fig.8), cannot provide the same quality for the excited power-like ones. Therefore in Figs.10 there are presented solely the results, achieved via direct numerical calculations. In Fig.10a with $\lambda = -0.9$ the lowest level is the exponential one, which approaches already for $h \simeq 7 a_B$ its asymptotic value $-0.5 Ha$, whereas three excited levels are power-like and tend very slowly to their common limiting point $-\lambda^2/2 = -0.405 Ha$. There is no intersection of levels, although for $h \simeq 8 a_B$ the ground state and the first excited one lie very close to each other. In Fig.10b for $\lambda = -1.2$ both the lowest level and the excited ones are power-like with the common limiting point $-\lambda^2/2 = -0.72 Ha$. Note that in the power-like case we avoid to classify the excited levels even in the asymp-

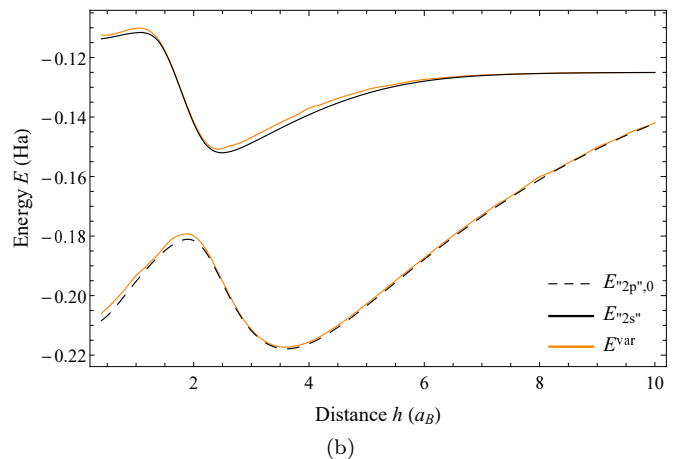
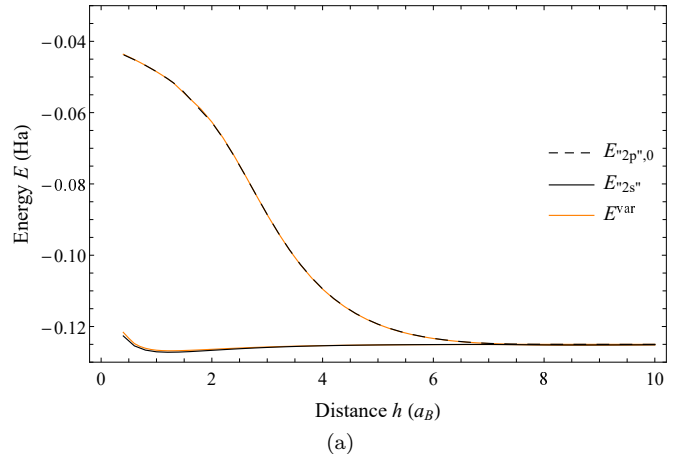


FIG. 9: (Color online). $E(h)$ for the first two excited levels with $m = 0$ for (a): $\lambda = 0.3$; (b): $\lambda = -0.3$. Variational estimates vs the results of direct numerical calculations.

totics for $h \rightarrow \infty$, since in $\mathbb{R}^3/2$ there remains only l_z as a conserved quantity, and hence, the levels cannot be labeled with definite values of the orbital moment. In addition, Figs.10 demonstrate quite explicitly the general property of the levels with power-like asymptotics that they approach their limiting point $(-\lambda^2/2)$ for $h \rightarrow \infty$ always much later than the exponential ones.

In Fig.11 the profile of the ground state $|\psi|^2$, considered as a function of z for $\rho = 0$, is shown for two quite representative values of $\lambda = -0.9, -1.2$, and two values of the nucleus position over plane $h = 3a_B, 10a_B$. In this case due to the axial symmetry the main contribution to the ground state WF should be formed by the planar s -wave component, and the choice $\rho = 0$ permits to consider indeed this dominating part of WF. From Fig.11 it is clearly seen that for $\lambda = -0.9$ and $h = 10a_B$, i.e. when the ground state is represented by an exponential level, $|\psi|^2$ is localized in the vicinity of the nucleus and is quite similar to the “normal” electronic ground state of free H. For the same λ and $h = 3a_B$ apart from the peak at the nucleus position there appears a tail, smeared over the boundary plane due to sufficiently strong attraction between the electron and the border. Actually, this tail underlies the emergence of power-like ground state levels

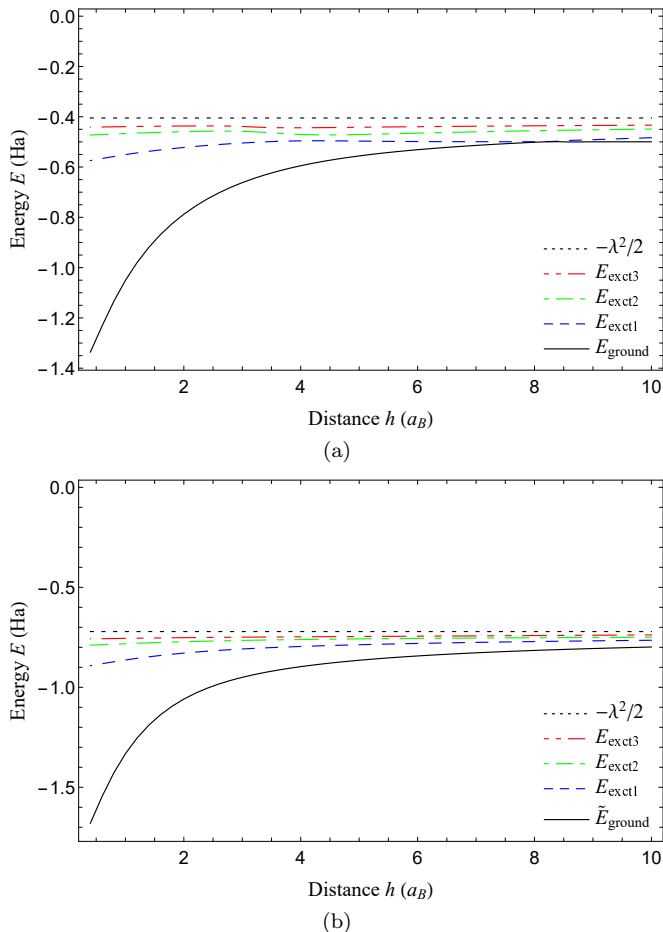


FIG. 10: (Color online). The dependence on h of four first levels with $m = 0$ for (a): $\lambda = -0.9$; (b): $\lambda = -1.2$. Various dashed colored curves correspond to direct numerical calculations for excited states, solid line denotes the ground state level, while the dotted line $= -\lambda^2/2$.

for $\lambda < -1$, whose structure, as it was already mentioned above, contains a large number of spherical harmonics in the form of a “drop” stuck and partially spread on the boundary plane. Therefore for $\lambda = -1.2$ the picture is quite different. In this case the ground state $|\psi|^2$ corresponds to a power-like level and is smeared in the vicinity of the border without any pronounced picks at the nucleus position. Another point is that the larger the nucleus position h over the plane, the more pronounced the spreading of $|\psi|^2$ over the boundary plane, since in the competition between electron-nucleus and electron-border interactions, the last one wins.

The dependence of the maximal ground state bound energy in the range $-1.5 < \lambda < 1$, where the minima of the energy curves are clearly visible (see Fig.8), is shown in Fig.12. There follows from the curve, representing this quantity at a given interval, that the general dependence on λ is nonlinear. For more negative λ the maximal bound state energy is reached for sufficiently more small distances $h \ll a_B$, when the electronic WF is localized in a small neighborhood of the boundary plane. In this

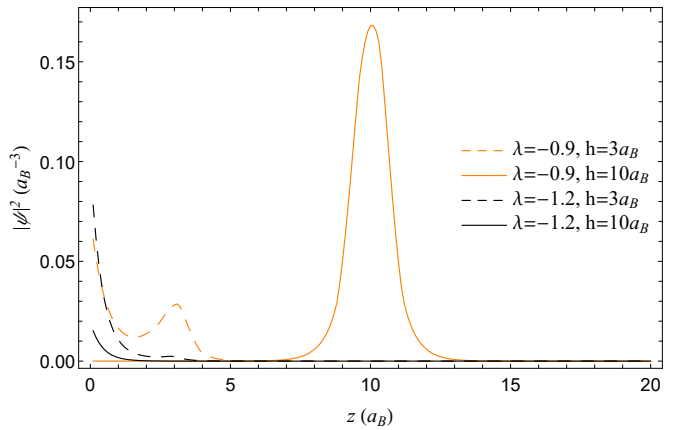


FIG. 11: (Color online). The profile of the ground state $|\psi|^2$ for $\rho = 0$.

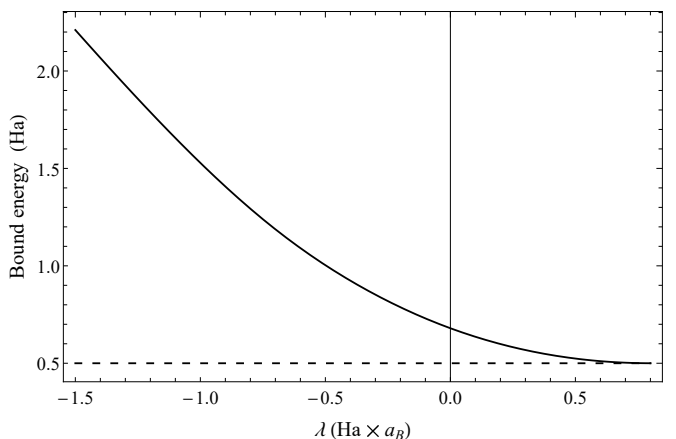


FIG. 12: The dependence of the ground state maximal bound energy on λ .

region the direct numerical calculations become cumbersome, and so the variational estimates via trial function come into play. The most pertinent trial function for the ground state of H with nucleus very close to the border is quite simple, namely

$$\psi_{\text{ground}}^{\text{tr}} = N^{-1/2} \exp(-|\lambda|z - \sigma r), \quad (62)$$

with N being the normalization coefficient

$$N = \frac{\pi}{4} \frac{|\lambda| + 2\sigma}{\sigma^2 (|\lambda| + \sigma)^2}, \quad (63)$$

while $\sigma > 0$ is the variational parameter. Such a choice for $\psi_{\text{ground}}^{\text{tr}}$ is automatically consistent with the boundary condition (4) and effectively describes the electronic state in the form of a “drop” stuck and partially spread on the border plane, that should be expected in the case of substantially negative λ .

Upon substituting (62) into (29) with $h \rightarrow 0$ we obtain a very simple expression for the mean value of the ground state energy

$$E_{\text{ground}}^{\text{tr}} = -\frac{\lambda^2}{2} + \frac{\sigma^2}{2} - 2\sigma \frac{|\lambda| + \sigma}{|\lambda| + 2\sigma}. \quad (64)$$

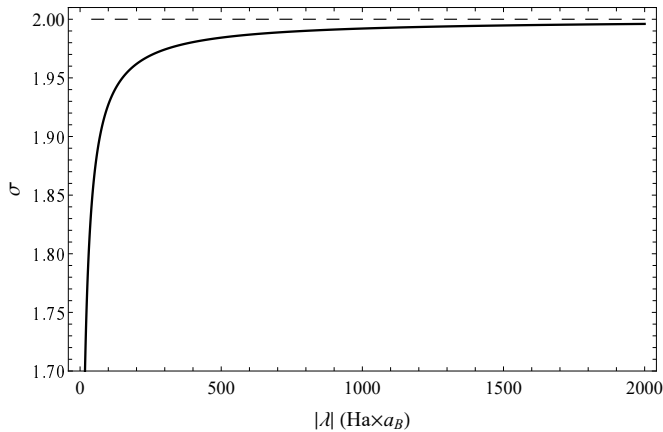


FIG. 13: The dependence on $|\lambda|$ of the parameter σ in ψ_{ground}^{tr} , which corresponds to the trial ground state with the maximal bound energy.

Variation of E_{ground}^{tr} yields the following equation for σ

$$4\sigma^3 + 4\sigma^2(|\lambda| - 1) + \sigma|\lambda|(|\lambda| - 4) - 2\lambda^2 = 0. \quad (65)$$

The eq. (65) possesses one real root, two remaining are complex. So from (65) we find for σ a unique answer in the form

$$\sigma = \frac{t}{6} + \frac{4|\lambda|^2 + 16|\lambda| + 16}{24t} + \frac{1 - |\lambda|}{3}, \quad (66)$$

where

$$t = (|\lambda|^3 + 33|\lambda|^2 + 12|\lambda| + 8 + 3\sqrt{3}\sqrt{2|\lambda|^5 + 39|\lambda|^4 + 24|\lambda|^3 + 16|\lambda|^2})^{1/3}. \quad (67)$$

Moreover, the expression (66) defines indeed the minimum of E_{ground}^{tr} , since there follows from (64), that E_{ground}^{tr} as a function of σ behaves like a distorted and shifted parabola. For $|\lambda| \gg 1$

$$\sigma \rightarrow 2 - \frac{8}{|\lambda|} + \frac{80}{|\lambda|^2} - \frac{960}{|\lambda|^3} + O\left[\frac{1}{|\lambda|}\right]^4. \quad (68)$$

The results for σ and the minimum of E_{ground}^{tr} , found this way, are shown in Figs.13-14 in dependence on $|\lambda|$. Remark, that in Fig.14 we present not E_{ground}^{tr} as itself, but the difference between E_{ground}^{tr} and the asymptotic value $E_{ground}(h \rightarrow \infty) = -\lambda^2/2$, namely

$$\Delta E^{tr} = E_{ground}^{tr} + \lambda^2/2. \quad (69)$$

This answer is physically more informative, since the main interest is indeed the shift of the ground state level for $h \rightarrow 0$ relative to the asymptotics for $h \rightarrow \infty$. For $|\lambda| \gg 1$

$$\Delta E^{tr} \rightarrow -2 + \frac{8}{|\lambda|} - \frac{64}{|\lambda|^2} + \frac{640}{|\lambda|^3} + O\left[\frac{1}{|\lambda|}\right]^4. \quad (70)$$

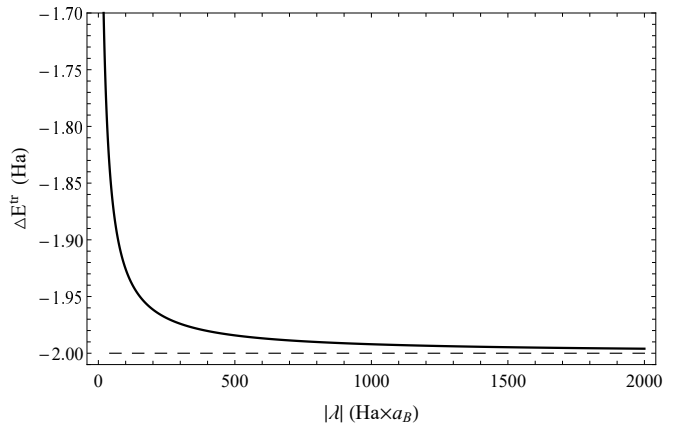


FIG. 14: The dependence on $|\lambda|$ of the trial ground state energy vs asymptotics for $h \rightarrow \infty$.

There follows from Fig.14 that for sufficiently negative λ or, equivalently, large positive electron-plane affinity, and $h \ll a_B$ the ground state level should lie more than $2Ha$ lower than its asymptotics far from the boundary. The corresponding energy curve, considered as a function of h , will be presented by a monotonic power-like one, interpolating these two asymptotics in a way, quite similar to the ground state curve shown in Fig.10b.

6. CONCLUSION

To summarize, we have shown that for a wide range of the “not going through the border” parameters the effective atomic potential, treated as a function of the distance h from H to the boundary plane, reveals in some cases a well pronounced minimum at certain finite but non-zero h , which corresponds to the mode of “soaring” of the atom over the plane. In other words, we obtain at the atomic level the microscopic version of the phenomenon called as the “Mahomet’s coffin” (such phenomenon is well-known in the superconductivity as one of the most prominent manifestations of the Meissner effect)¹. However, it would worth to emphasize that due to the boundary surface roughness such an effect can be an observable one only in those cases when the distance between the energy minimum and the surface is not less than a_B . Otherwise, such minima will be indistinguishable against the background of inhomogeneities in atomic layers on the boundary surface. At the same time, when such a minimum of atomic level is located at a sufficient distance from the surface (as in Figs.2,4,5,7,9), so that its roughness becomes insignificant, the soaring mode could take place. The atom in this mode is able to move freely par-

¹ To avoid disappointing misunderstandings and speculations the authors would like to underline that the terminology used has long been adopted to denote such a physical effect of soaring over a plane and has nothing to do with theological views.

allel to the boundary plane with an arbitrary wavevector \vec{K}_{\parallel} . If this movement can be stopped, there appears a specific version of a Penning trap for atomic H without complicated 3-dimensional configuration of external fields. The stability of such “soaring” states depends on the overlap of their electronic WF’s, since each WF should be more or less located in the vicinity of the nucleus position at the minimum of the corresponding energy curve, and for well pronounced energy minima could be quite high.

Now let us turn to the general features of the power-like levels, which for sufficiently large positive affinity of the atom to the boundary plane, i.e. for $\lambda \leq -1$, turn out to be the lowest ones, and hence, the most important. First it should be mentioned that although in these states the electronic WF is located mostly in the vicinity of the border, these levels are principally different from the other known single-electron surface states. Between the latter in the first place there are the Tamm states, which arise on the surface of the crystal solids of finite size (see, e.g., Ref.[58] and citations therein). But their emergence is intimately connected with the intrinsic structure of the medium, whereas the origin of the power-like levels is the result of specific interplay between the Robin boundary condition on the border and the electron-nucleus electrostatic interaction outside the medium. More closer in nature to the power-like levels there are the “surface-localized states”, considered in Ref.[59], since their appearance is also caused by the electrostatic interactions in the system. In this case the crucial role is played by the interaction between the atom and medium, filling the half-space $z < 0$, when the dielectric properties of the latter are taken into account. Namely, when the dielectric constant ε of the medium is large, for $h \ll a_B$ the superposition of the atomic potentials and the dielectric response of medium leads to a potential similar to that of the “one-dimensional hydrogen atom” [60, 61] in z-direction

$$V_S(z) = -\gamma(\varepsilon)/4z, \quad (71)$$

where $\gamma(\varepsilon) = (\varepsilon - 1)/(\varepsilon + 1) \simeq 1$ for $\varepsilon \gg 1$. However, the interpretation of this result is ambiguous, since the corresponding spectral problem is not self-adjoint and requires additional restrictions to provide a self-adjoint extension, which is in principle not unique [62]. In Ref.[59] there was proposed the solution by means of the Dirichlet condition on the surface $z = 0$ (it is so-called Loudon’s extension). In this case the potential (71) yields the single-electron “surface-localized states”, which are capable of free motion parallel to the surface, but localized in z-direction in the vicinity of the boundary plane with bound energies

$$\mathcal{E}_n = -\gamma(\varepsilon)^2/32 n^2 \simeq -0.85\gamma(\varepsilon)^2/n^2 \text{ eV}, \quad n = 1, 2 \dots \quad (72)$$

However, such a picture has nothing to do with the power-like levels, since it emerges only for $\lambda \rightarrow \infty$ and only if the nucleus approaches the border, i.e. when

$h \rightarrow 0$. To the contrary, the power-like levels appear in the case of Robin condition with $\lambda < 0$ and exist for any $0 \leq h \leq \infty$. It should be also mentioned that the combination of the Robin condition with the potential (71) requires a separate consideration without going to the limit $h \rightarrow 0$.

At the same time, indeed these power-like levels define the effective atomic H potential in the case of a large positive affinity. The most important properties of this potential are the following. First, it is strictly attractive and long-range, since these levels tend to their limiting values very slow, actually as $\sim 1/h$, in contrast to the van der Waals potential $V_A(h)$ between neutral atoms, which falls down as $\sim 1/h^6$. In Refs.[30, 31] it was shown that even for the first critical $\lambda_{crit,1} = -1$, when the limiting value of the lowest power-like level coincides with E_{1s} , such a state should be energetically favorable compared to the free atom up to actual nanocavities with sizes $\sim 100 - 1000$ nm. Another attractive feature is that although such levels don’t provide well-pronounced minima at $h \gtrsim a_B$, for small $h \ll a_B$ their bound energy could exceed several Ha (see Figs.10,12,14). Therefore, when H in such a power-like state moves from the region $h \gg a_B$ to the border, a significant amount of energy can be released, the more, the closer to the border the nucleus could be, that can be achieved for sufficiently negative λ or, equivalently, large positive affinity. The magnitude of this energy release, as it follows from Fig.14, should be estimated as not less than $2Ha$. Moreover, this effect can be sufficiently enhanced by the fact that the attraction of atoms to the plane will be long-range, and hence, the number of atoms involved in this process can be quite large. It would be worthwhile to note that in a more realistic situation an important role should be played by the degree of roughness of the boundary surface, since it determines how close the atom can approach the border and, simultaneously, it influences the magnitude of the affinity and so the value of λ . In any case, however, it can be assumed that for a fresh sample with a clean smooth surface and a very low initial H-concentration inside, hence, with a large positive affinity to H, in the first stages of hydrogenation the energy release can be such that it could explain the known events of thirty years ago (the authors believe that their hint is transparent enough to do it without references).

Finally, it should be mentioned that here we consider a model stationary picture, which ends with the adsorption of H on the boundary plane. In a more realistic situation the process continues further in the form of physi/chemisorption through the boundary surface, for which it is necessary to introduce into λ an imaginary part to provide the non-vanishing current through the border. In this case we should deal with a non-stationary picture in terms of inelastic process with metastable states, which imply another techniques including complex energies and Jost functions and therefore will be considered separately.

-
- [1] W. Jaskolski, *Phys. Repts.* **271**, 1 (1996).
- [2] E. J. Sabin and E. Brandas, *Theory of Confined Quantum Systems*, Adv. in Quant. Chem., Vol. 57-58 (Academic Press, 2009).
- [3] K. Sen, *Electronic Structure of Quantum Confined Atoms and Molecules* (Springer International Publishing, 2014).
- [4] E. Wigner and F. Seitz, *Phys. Rev.* **43**, 804 (1933).
- [5] E. Wigner and F. Seitz, *Phys. Rev.* **46**, 509 (1934).
- [6] A. Sommerfeld and H. Welker, *Ann. Phys.* **424**, 56 (1938).
- [7] A. Michels, J. D. Boer, and A. Bijl, *Physica* **4**, 981 (1937).
- [8] J. D. Levine, *Phys. Rev.* **140**, A586 (1965).
- [9] Z. Liu and D. L. Lin, *Phys. Rev. B* **28**, 4413 (1983).
- [10] A. F. Kovalenko, E. N. Sovyak, and M. F. Holovko, *Int. J. Quant. Chem.* **42**, 321 (1992).
- [11] Y. Shan, T.-F. Jiang, and Y. C. Lee, *Phys. Rev. B* **31**, 5487 (1985).
- [12] S. A. Cruz, E. Ley-Koo, and R. Cabrera-Trujillo, *Phys. Rev. A* **78**, 032905 (2008).
- [13] R. Méndez-Fragoso and E. Ley-Koo, *Int. J. Quant. Chem.* **111**, 2882 (2011).
- [14] E. Ley-Koo and R. Garcia-Castelan, *J. Phys. A* **24**, 1481 (1991).
- [15] S. A. Cruz, E. Ley-Koo, J. L. Marin, and A. Taylor-Armitage, *Int. J. Quant. Chem.* **54**, 3 (1995).
- [16] E. Ley-Koo and K. P. Volke-Sepúlveda, *Int. J. Quant. Chem.* **65**, 269 (1997).
- [17] E. Ley-Koo and S. Mateos-Cortés, *Int. J. Quant. Chem.* **46**, 609 (1993).
- [18] E. Ley-Koo and S. Mateos-Cortés, *Am. J. of Phys.* **61**, 246 (1993).
- [19] L. Chaos-Cador and E. Ley-Koo, *Int. J. Quant. Chem.* **103**, 369 (2005).
- [20] Y. Shan, *J. Phys. B* **23**, L1 (1990).
- [21] A. F. Kovalenko and M. F. Holovko, *J. Phys. B* **25**, L233 (1992).
- [22] S. Wethekam, D. Valdés, R. C. Monreal, and H. Winter, *Phys. Rev. B* **78**, 075423 (2008).
- [23] R. Monreal, D. Goebel, D. Primetzhofer, and P. Bauer, *Nucl. Instr. and Methods in Phys. Research B* **315**, 206 (2013), 25th Int. Conf. on Atomic Collisions in Solids (ICACS-25).
- [24] V. Pupyshev, *Rus. J. of Phys. Chem. A* **74**, 50 (2000).
- [25] K. Sen, V. Pupyshev, and H. Montgomery, *Adv. in Quant. Chem.*, **57**, 25 (2009).
- [26] M. Al-Hashimi and U.-J. Wiese, *Ann. Phys.* **327**, 1 (2012).
- [27] M. Al-Hashimi and U.-J. Wiese, *Ann. Phys.* **327**, 2742 (2012).
- [28] K. A. Sveshnikov and A. V. Tolokonnikov, *Moscow University Phys. Bull.* **68**, 13 (2013).
- [29] K. A. Sveshnikov and A. A. Roenko, *Phys. Part. Nucl. Lett.* **10**, 398 (2013).
- [30] K. A. Sveshnikov, *Theor. Math. Phys.* **176**, 1044 (2013).
- [31] K. Sveshnikov and A. Roenko, *Physica B* **427**, 118 (2013).
- [32] V. I. Pupyshev and A. V. Scherbinin, "Symmetry Reduction and Energy Levels Splitting of the One-Electron Atom in an Impenetrable Cavity," in *Electronic Structure of Quantum Confined Atoms and Molecules*, edited by K. Sen (Springer International Publishing, Cham, 2014) pp. 31–58.
- [33] K. Sveshnikov and A. Tolokonnikov, *Eur. Phys. J. D* **71**, 193 (2017).
- [34] K. A. Sveshnikov, P. K. Silaev, and A. V. Tolokonnikov, *Moscow University Phys. Bull.* **72**, 29 (2017).
- [35] R. Caputo and A. Alavi, *Mol. Phys.* **101**, 1781 (2003).
- [36] K. Christmann, *Surface Science Repts.* **9**, 1 (1988).
- [37] A. Züttel, *Materials Today* **6**, 24 (2003).
- [38] Y. Fukai, *The Metal-Hydrogen System. Basic Bulk Properties*, Springer Series in Materials Science, Vol. 21 (Springer-Verlag Berlin Heidelberg, 2005) pp. 1–500.
- [39] K. Christmann, *Surface Science* **603(10-12)**, 1405 (2009).
- [40] M. Wilde and K. Fukutani, *Surface Science Repts.* **69**, 196 (2014).
- [41] E. Callini, S. Kato, P. Mauron, and A. Züttel, *CHIMIA Int. Journ. for Chemistry* **69**, 269 (2015).
- [42] D. Stolten and B. Emonts, eds., *Hydrogen Science and Engineering : Materials, Processes, Systems and Technology*, Wiley Online Library (Wiley-VCH Verlag GmbH & Co. KG & A, 2016) pp. 1–1138.
- [43] B. Hammer, Y. Morikawa, and J. K. Nørskov, *Phys. Rev. Lett.* **76**, 2141 (1996).
- [44] M. Pedersen, S. Helveg, A. Ruban, I. Stensgaard, E. Lægsgaard, J. Nørskov, and F. Besenbacher, *Surface Science* **426**, 395 (1999).
- [45] V. Pallassana, M. Neurock, and G. W. Coulston, *Journ. Phys. Chem. B* **103**, 8973 (1999).
- [46] V. Pallassana, M. Neurock, L. B. Hansen, and J. K. Nørskov, *J. Chem. Phys.* **112**, 5435 (2000).
- [47] J. Greeley and M. Mavrikakis, *Journ. Phys. Chem. B* **109**, 3460 (2005), pMID: 16851380.
- [48] E. Tosatti and N. Manini, *Chem. Phys. Lett.* **223**, 61 (1994).
- [49] M. Amusia, A. Baltenkov, and B. Krakov, *Phys. Lett. A* **243**, 99 (1998).
- [50] H. Bateman and A. Erdélyi, *Higher transcendental functions*, Vol. 1-2 (McGraw-Hill, 1953).
- [51] J. von Neumann and E. Wigner, *Phys. Zeitschrift* **30**, 465 (1929).
- [52] J. von Neumann and E. Wigner, *Phys. Zeitschrift* **30**, 467 (1929).
- [53] L. Landau and E. Lifshitz, *Quantum Mechanics Non-Relativistic Theory, Third Edition: Volume 3 (Course of Theoretical Physics) (Vol. 3) 3rd Edition* (Pergamon Press, NY, 1981) pp. 1–673.
- [54] I. V. Komarov, L. I. Ponomarev, and S. Y. Slavyanov, *Spheroidal and Coulomb Spheroidal Functions (in Russian)* (Nauka, Moscow, USSR, 1976).
- [55] C. Itzykson and J.-B. Zuber, *Quantum Field Theory* (Courier Corporation, 2012) pp. 1–752.
- [56] P. G. Ciarlet, *The finite element method for elliptic problems* (Elsevier North-Holland Amsterdam, New York, 1978) pp. 1–530.
- [57] F. Bechstedt, *Principles of Surface Physics*, Advanced texts in physics (Springer-Verlag Berlin Heidelberg NewYork, 2012) pp. 1–341.
- [58] M. Cottam and D. Tilley, *Introduction to surface and superlattice excitations*, Graduate Student Series in Physics (IOP Publishing Ltd, Bristol and Philadelphia, 2005) pp. 1–511.
- [59] M. Babiker and D. R. Tilley, *Proc. Roy. Soc. A* **378**, 369

- (1981).
- [60] R.Loudon, *Am. J. of Phys.* **27**, 649 (1959).
- [61] R.J.Elliott and R.Loudon, *Journ. Phys. Chem. of Solids* **15**, 196 (1960).
- [62] D. M. Gitman, I. V. Tyutin, and B. L. Voronov, *Self-adjoint Extensions in Quantum Mechanics : General Theory and Applications to Schroedinger and Dirac Equations with Singular Potentials*, Progress in Mathematical Physics , 62 (Springer Science & Business Media, 2012) pp. 1–511.